

Abstract

Ali Soheil Sadri: Novel Adaptive Power and Rate Control in Third Generation Wideband CDMA Mobile Systems, under the direction of Dr. Winser Alexander.

This Dissertation proposes novel adaptive power control and rate change schemes and investigates the performance of a Wideband Code Division Multiple Access (W-CDMA) system in conjunction with these adaptive techniques. In these schemes, the transmit power and rate are adapted to the variations of the fading channel using adaptive thresholds based on the probability distribution function (pdf) of the predicted mobile channel power values.

We define a policy similar to the traditional power control technique with thresholds except that the thresholds are set based on several regions of operation in our Adaptive Transmitter Power Control (TPC) and Adaptive Seamless Rate Change (SRC) schemes. These regions are defined by means of the probability distribution function (pdf) of the total average channel power. The pdf is initially constructed based on the history of the predicted channel power values derived from the long-range prediction algorithm. These regions can be defined such that the system operates at a constant ratio of energy per bit over noise power.

In a 1-user model with one channel path, the pdf of the channel power would be an exponential or chi-square function with 2 degrees of freedom. However, in a W-CDMA system, normally the rake receiver has several fingers. That is, at the receiver, the system either estimates or predicts the channel coefficients at each rake finger and performs maximal ratio combining by multiplying each finger with its conjugate or

chooses the ones with the highest energy and performs maximal ratio combining on the selected fingers.

In a two-user system where the multi-access interference is modeled as the Standard Gaussian Approximation (SGA), the system performance and error probability of our W-CDMA system becomes similar to the one for our one-user system. Consequently, in a single user detector system, when all users adopt a similar policy for their adaptive power and rate control, the average total Multi-Access Interference (MAI) will be reduced. The resulting channel capacity of the system in this case will be increased and the system may operate in a lower transmit power level.

We evaluate the performance of these schemes using a detailed block diagram simulation of a W-CDMA system. We model and simulate all major components of the system including an accurate model for realistic mobile channels. We present simulation results to verify that the proposed novel schemes are superior to the traditional approaches for transmitter power control and rate change. Furthermore, our simulation results show that our proposed techniques reduce the effect of Multi Access Interference in a multi-user system.

Novel Adaptive Power and Rate Control in Third Generation Wideband CDMA Mobile Systems

By:

ALI SOHEIL SADRI

A Dissertation Submitted to the Graduate Faculty of
the North Carolina State University
in Partial Fulfillment of the
Requirement for the Degree of
Doctoral of Philosophy

Department of Electrical and Computer Engineering

Raleigh, North Carolina

April 27, 2000

Approved by:

Dr. Winser Alexander, Chairman

Dr. Brian Hughes, Member

Dr. Ernest Stitzinger, Member

Dr. Andy Rindos, Member

This dissertation is dedicated to my father, Gholamali Sadri (1917-1996)

BIOGRAPHY

Ali Soheil Sadri was born in March 10, 1964 in Tehran, Iran. After obtaining his high school diploma, he moved to the United States in 1985 to continue his studies at the Tennessee Technological University (TTU) in Cookeville, Tennessee. In the summer of 1986, Ali transferred to North Carolina State University (NCSU) in Raleigh, North Carolina. In the fall of 1989, he completed his undergraduate degree and immediately entered the graduate program in Electrical Engineering. Ali obtained his Masters degree in 1991 while working at IBM in Research Triangle Park, North Carolina. During his employment at IBM, he was involved in development of several products including modems, echo cancellers, tone detectors and speech coders. While working at IBM, he attended the Doctoral program at NCSU as a part time student. In 1995, Ali became Program Manager of Telecommunications Standards at IBM, which he became an active member of the Telecommunications Industry Association (TIA) and International Telecommunications Union (ITU) standards committees. In December 1999, Ali joined Billions of Operation Per Second Inc. (BOPS) where he is currently Director of Communications Development.

ACKNOWLEDGEMENTS

I remember the very first day I wanted to go to school thirty years ago. I was frightened and reluctant. I remember the days that the kids were getting punished for their naughtiness in the elementary school next to our house in Tehran. I remember my fear of going to school by myself. I remember my tears associated with not wanting to go to school. I remember the days that my father tried to convince me that school is not as terrifying as I believed it was. I remember the days that my mother felt responsible to take me to school and stay with me in the classroom in first grade.

Thirty years ago, I would not have imagined that one day I would be called Dr. Ali Soheil Sadri. With this note, I would like to acknowledge several individuals that helped me to be the person I became today.

I would like to thank my deceased father, Golamali Sadri. He was the man who spent all his life in providing the best of everything for us. He is not here with me, but I am sure he would have been proud of me if I could have heard him. I would like to thank my mother, Fatemeh Mirfakraie, because without her persistence and dedications I would not have become the person that I am today. I would like to thank my Sisters, Susan and Afsaneh Kokab Sadri, who helped me with their support and love during my teenage years in Iran. I would like to thank my elder brother Ali Saeid Sadri for his helpful recommendations during the early years of my life in the United States. I also would like to acknowledge my eldest brother Ali Massoud Sadri for his financial commitment to me because I would not have been able to come to the United States and pursue my higher education without his help. I would like to acknowledge my beautiful wife, Behrokh

Bagherifar Sadri, for her dedication and endless love to me that enabled me with the extra power I needed to complete my Ph. D. I would like to thank my unborn child, which my wife is carrying, for keeping my spirit happy and strong.

I would like to acknowledge my advisory committee members, Dr. Brian Hughes, Dr. Ernest Stitzinger, Dr. Andy Rindos and my special thanks to my advisor Dr. Winsor Alexander who supported me very strongly throughout the last two years of my research studies and made constructive recommendations to help me to complete my Ph. D.

I also would like to thank my colleagues at IBM, especially my former Director Richard Warren, who supported me during the last two years to complete my dissertation. Finally, I would like to acknowledge my other friends and family who I have not mentioned in this note for their support and understanding.

I thank God for all he has given to me. This has been a beautiful and unforgettable experience in my life. I hope that I would be capable of paying my share to human kind with all the knowledge I have learned and will learn during my life.

TABLE OF CONTENTS

LIST OF FIGURES.....	viii
-----------------------------	-------------

LIST OF TABLES.....	x
----------------------------	----------

1 Introduction.....	1-2
----------------------------	------------

1.1 BACKGROUND LITERATURE.....	1-3
1.2 PRIOR ART PATENT DISCLOSURES	1-6
1.3 PROBLEM DEFINITION	1-9
1.4 RESEARCH CONTRIBUTION	1-10

2 Propagation, Characterization and Long Range Prediction of the Mobile Channel	2-15
--	-------------

2.1 MOBILE CHANNEL CHARACTERIZATION FUNCTIONS	2-16
2.2 FADING CHANNELS	2-20
2.2.1 Flat Fading Due to Delay Spread.....	2-21
2.2.2 Frequency Selective Fading Due to Delay Spread	2-22
2.2.3 Slow and Fast Fading Due to Doppler Spread	2-23
2.3 RAYLEIGH FADING MODEL.....	2-25
2.4 LONG RANGE CHANNEL PREDICTION.....	2-28
2.5 CHANNEL POWER PREDICTION.....	2-30

3 Multiple Access Technology	3-33
---	-------------

3.1 FREQUENCY DIVISION MULTIPLE ACCESS (FDMA)	3-33
---	------

3.2	TIME DIVISION MULTIPLE ACCESS (TDMA)	3-34
3.3	CODE DIVISION MULTIPLE ACCESS (CDMA)	3-36
3.4	WIDEBAND CDMA SYSTEM.....	3-39
3.4.1	W-CDMA Physical Channel Structure	3-41
3.4.2	Orthogonal Variable-Length Code.....	3-43
3.4.3	Multiple Spreading.....	3-45
3.4.4	Closed-Loop Power Control	3-45
4 Novel Adaptive Power and Rate Control Techniques with Analytical Results.....		4-49
4.1	ADAPTIVE POWER AND RATE CONTROL.....	4-51
4.2	GENERAL PROCEDURE.....	4-54
4.2.1	Transmitter Power Control (TPC)	4-54
4.2.2	Seamless Rate Change (SRC)	4-55
4.3	ANALYTICAL RESULTS IN FLAT RAYLEIGH FADING CHANNEL	4-57
4.4	ANALYTICAL RESULTS IN MULTIPATH RAYLEIGH FADING CHANNEL.....	4-62
4.5	ANALYTICAL RESULTS FOR MULTI-USER PERFORMANCE.....	4-68
5 Simulations Results		5-75
5.1	FLAT FADING PERFORMANCE	5-84
5.2	MULTIPATH FADING PERFORMANCE	5-87
5.3	MULTI-USER PERFORMANCE.....	5-91
6 Conclusion and Future Work.....		6-98
7 References.....		7-102

LIST OF FIGURES

FIGURE 2.1. GENERAL MOBILE CHANNEL MODEL.....	2-16
FIGURE 2.2. K-PATH CHANNEL MODEL.....	2-18
FIGURE 2.3. GENERAL RELATIONSHIP BETWEEN THE CHANNEL CHARACTERIZATION FUNCTIONS.....	2-20
FIGURE 2.4. TYPICAL MULTIPATH ENVIRONMENT.....	2-21
FIGURE 2.5. FLAT FADING CHANNEL CHARACTERISTICS.....	2-22
FIGURE 2.6. DOPPLER EFFECT.....	2-23
FIGURE 2.7. RAYLEIGH FADING ENVELOPE AT 4.096 MCPS.....	2-26
FIGURE 2.8. TWO-RAY MULTIPATH CHANNEL MODEL.....	2-27
FIGURE 3.1. GRAPH OF THE TIME DOMAIN VS FREQUENCY DOMAIN OF THE FDMA SYSTEM.....	3-34
FIGURE 3.2. GRAPH OF THE TIME DOMAIN VS FREQUENCY DOMAIN OF THE TDMA SYSTEM.....	3-35
FIGURE 3.3. GRAPH OF THE TIME DOMAIN VS FREQUENCY DOMAIN AND CODEWORD OF THE CDMA SYSTEM.....	3-37
FIGURE 3.4. SPECTRUM OF WCDMA COMPARED TO THE FCDMA.....	3-39
FIGURE 3.5. UPLINK CHANNELIZATION AND SCRAMBLING.....	3-41
FIGURE 3.6. UPLINK W-CDMA FRAME STRUCTURE.....	3-42
FIGURE 3.7. OVVSF CODE TREE.....	3-44
FIGURE 3.8. CLOSED-LOOP POWER CONTROL STRUCTURE AT THE BASE STATION.....	3-46
FIGURE 4.1. THREE-REGION PDF OF THE CHANNEL POWER.....	4-53
FIGURE 4.2. ORTHOGONAL CODE CHANGE SCHEME.....	4-56
FIGURE 4.3. THEORETICAL PE VS. EB/N0 WITH/WITHOUT TPC/SRC 1-DB ADJUSTMENT	4-60
FIGURE 4.4. THEORETICAL PE VS. EB/N0 WITH AND WITHOUT TPC/SRC WITH 3-DB ADJUSTMENT.....	4-61
FIGURE 4.5. CHANNEL POWER PDF FOR 1, 2, 3 AND 4 PATHS.....	4-64
FIGURE 4.6. THEORETICAL PE VS. EB/N0 WITH/WITHOUT TPC/SRC, 1, 2, & 4 PATHS.....	4-67
FIGURE 4.7. BER PERFORMANCE IN MULTI USER SYSTEM, EXACT AND GAUSSIAN APPROXIMATION.....	4-71

FIGURE 5.1. BLOCK DIAGRAM OF SIMULATION TOPOLOGY FOR W-CDMA SYSTEM	5-75
FIGURE 5.2. RATE $\frac{1}{2}$ CONVOLUTIONAL ENCODER	5-76
FIGURE 5.3. BLOCK INTERLEAVING	5-77
FIGURE 5.4. BAND PASS FADING CHANNEL MODEL BLOCK DIAGRAM.....	5-78
FIGURE 5.5. RECEIVER BLOCK DIAGRAM.....	5-80
FIGURE 5.6. OPTIMUM MRC FOR BPSK SIGNALING	5-81
FIGURE 5.7. GENERAL BLOCK DIAGRAM OF MS OR BS RECEIVER OPERATING IN TPC/SRC MODE	5-83
FIGURE 5.8. EXPERIMENTAL PE VS. EB/N0 WITH/WITHOUT TPC/SRC	5-85
FIGURE 5.9. COMPARISON OF THE SIMULATION AND THE THEORETICAL RESULTS FOR 1 PATH.....	5-86
FIGURE 5.10. BAND PASS FADING CHANNEL MODEL BLOCK DIAGRAM.....	5-87
FIGURE 5.11. SIMULATION RESULTS FOR PE VS. EB/N0 WITH/WITHOUT TPC/SRC, 2- PATHS	5-89
FIGURE 5.12. COMPARISON OF THE SIMULATION AND THE THEORETICAL RESULTS FOR 2 PATHS	5-90
FIGURE 5.13. TOP LEVEL BLOCK DIAGRAM OF A 2-USER W-CDMA SYSTEM	5-92
FIGURE 5.14. BAND PASS FADING CHANNEL MODEL WITH MAI	5-93
FIGURE 5.15. SIMULATION RESULTS FOR PE VS. EB/N ₀ , 2-USER PERFORMANCE, CONSTANT POWER USER 1	5-94
FIGURE 5.16. SIMULATION RESULTS FOR PE VS. EB/N ₀ , 2-USER PERFORMANCE, EQUAL POWER	5-95

LIST OF TABLES

TABLE 3.1. CDMA SYSTEM FEATURES AND LIMITATIONS	3-38
TABLE 3.2. W-CDMA MODULATION PARAMETERS	3-40

Chapter One: Introduction

1 Introduction

In wireless communication systems, signal fading due to multipath radio propagation severely degrades the performance and imposes high transmitter power requirements. Since the characteristics of the mobile channel changes rapidly, the transmitter and the receiver cannot be configured to operate at their optimum performance levels and therefore, they fail to exploit the full potential of the wireless system. One of the advantages of the CDMA system is that it increases the capacity of the channel due to the fact that each user in the system occupies the entire frequency band and therefore there is no waste of bandwidth due to channel spacing. In this study, we concentrate on the mitigation of fading effects in the third generation wireless systems. The most popular system under study is the Wideband CDMA (W-CDMA) [1,2,3].

Clear voice service, high-speed mobile Web surfing, video conferencing from anywhere in the world, and thousands of other advanced applications over the wireless phone or handheld PC are the visions of the developers of the third generation wireless system [4]. Generally, any enhancements to the system that can improve the delivery of high-speed data, voice and video over mobile devices while increasing the battery life are challenging topics for consideration. In this regard, transmitter power control and adaptive rate change are popular topics of interest for researchers.

In the absence of power control, a Base Station (BS) would receive a much stronger signal from a Mobile Station (MS) that is geographically close to it than from a MS that is farther away. This is so called the near-far problem. In this case, power control schemes on the up-link or the reverse-link attempt to adjust the transmitted power

of each MS so that the nominal received power from each MS to the BS is almost the same.

1.1 Background Literature

Several authors have proposed techniques for adaptive modulation, adaptive power control, and adaptive coding. Adaptive modulation, which requires accurate channel estimation at the receiver and a reliable feedback information path between the receiver and the transmitter, had initially been discussed in the 1960's [5]. The basic idea behind any adaptive transmission is to maintain a constant ration of energy per bit over noise power E_b/N_0 at the receiver by varying the transmitter power level or adjusting the transmitted rate or coding. The issue of adaptive modulation has become an important topic of interest for many researchers in recent years due to the need for higher and more reliable communication systems.

For example, Alouini and Goldsmith in one of their recent studies examined the capacity of Rayleigh fading channels under different adaptive transmission techniques [6]. The authors in this paper study the Shannon capacity of adaptive transmission techniques where they consider both the Maximum Ratio Combining (MRC) and Selective Combining (SC) of the received signal. This paper presents a policy of outage probability where no data is transmitted during low signal power reception at the receiver. The authors assume a very slow flat fading channel in this research. They also state in the paper that when both adaptive power and rate control is applied in a system, the combination yields a small increase in system capacity.

In another paper, Alouini et al. propose an adaptive modulation technique for simultaneous voice and data transmission over fading channels [7]. In this work, they

illustrate a technique to dynamically allocate the transmitted power between the Inphase (I) and Quadrature (Q) channels. This technique uses fixed-rate Binary Phase Shift Keying (BPSK) modulation on the “ Q ” for the voice channel and variable rate M-ray Amplitude Modulation (AM) on the “ I ” channel for data. As the channel degrades, the modulation gradually reduces its data throughput and reallocates most of the power to insure a continuous and satisfactory voice transmission.

Power control is vital in wireless communications. It mitigates the effects of the fading channel and also inherently lowers the power consumption if managed correctly. Lower transmit power yields a reduction in the Multiple Access Interference (MAI) and consequently increases channel capacity.

Among papers on power control, there is a study by Lee and Steel [8]. The authors in this paper suggest a fixed-step and an adaptive-step closed-loop power control scheme that makes use of the multitap RAKE receivers for tracking the power variation due to path loss and fading. The authors state that the measurement of the received signal power and the ratio of the bit energy-to-interference power spectral density play an important role in the accuracy of the CDMA power control.

The performance of closed-loop power control in CDMA systems is a very attractive and critical research topic and several authors such as Sim et al. have presented important contributions [9]. They show that the fast closed-loop power control algorithm functions effectively when the speed of the mobile unit is in the range such that its Doppler frequency is less than one tenth of the power control update rate.

Along with the study of the closed-loop power control is the study of the predictive power estimators in CDMA systems. J. Tanskanen et al. suggest a Wiener

model based upon computationally effective power estimators (PE) for complex signals. The PEs in their proposal were designed to be one-step-ahead predictive and they found that a short filter between 5 to 21 taps was adequate [10].

Another related study in power control is the suggestion for a dynamic, combined power control and forward error correction control (FEC) algorithm for the mobile radio system that can minimize the power consumption at the transmitter while increasing the number of users. P. Agrawal et al. propose the use of feedback of the target word-error-rate at the receiver to adjust their transmitter power [11].

The combination of the rate, gain and coding change schemes through the use of the feedback transmission of the information from the BS to the MS are all interesting studies that claim to improve the performance of the mobile channel [12, 13]. In these proposals, which are similar to the other proposals, the authors propose that the quality of the channel can be determined on the basis of the calculation of the short-term signal to interference plus noise ratio $C/(N_0 + I_0)$ at the BS receiver.

A combination of an adaptive coding rate and process gain control technique has been presented as an effective technique in enhancing the performance of the mobile radio system. S. Abeta et al. describe a CDMA based radio subsystem for multi-media commercial communication services that includes a channel activation function for different multimedia type applications [14]. This includes two types of media, i.e. fixed size data such as computer data and still images, and constant bit rate data such as voice and video. The system achieves high throughput data transmission for the fixed size data by controlling the process gain and coding rate according to the variation of the channel. When the instantaneous received carrier power-to-noise plus interference spectral density

is low, low coding rate and large process gains are selected to improve transmission quality whereas high coding rate and small process gains are selected to achieve the higher bit rate when the instantaneous spectral density ratio is low. For the constant bit rate data, a channel activation technique was disclosed in which the data are transmitted in a shorter burst when the bit rate is high and transmitted in a longer burst when the bit rate is low to keep its bit rate constant.

Sampei et al. propose a wireless packet transmission scheme with adaptive processing gain and power control techniques for circuit-switched and packet-switched mode integrated DS-CDMA systems [15]. The authors suggested in this paper that the proposed algorithm dynamically control the power and rate of the two integrated systems at the Base Station according to the channel load.

The main purpose of the schemes presented in these papers is the maximization of data throughput using a limited bandwidth while keeping transmission quality constant. However, in practice, the channel is time-variant due to fast fading and current measurements are not sufficient and adequate for determining the adaptation scheme for the next frame [16].

1.2 Prior Art Patent Disclosures

There have been several patent disclosures that address the power control for CDMA systems. We have examined several U.S and international patent disclosures to validate the novelty of our proposed techniques and we present a summary of the relevant discussions in this section.

In one invention, E. Tiedemann et al. discuss a method and apparatus for controlling transmission power in a variable rate communication system [17]. The

method disclosed provides for a closed loop power control method. A first remote station controls the transmission power of a second remote station by transmitting a rate dependent power control signal to the second remote communications system. Since only the second communications system knows its transmission rate a priori, it must determine a course of action in accordance with both the received power control signal and the knowledge of its transmission rate.

In another patent, L. Weaver et al. discloses an apparatus and method for controlling a final transmit power, Y of a base station in a cellular communications system that has several channels [18]. The base station has a transmitter power tracking gain Y and a radio frequency transmit power W . The apparatus comprises channel elements for calculating expected power that is the received power minus the transmitted power for each of corresponding channels. The apparatus also comprises a Base-station Transceiver System Controller (BTSC) for generating a desired output power, Y_d for the base station including an adder for summing the expected powers. The apparatus also includes a transmit power detector for measuring Y to obtain the measured transmit power. The apparatus further comprises a Radio Frequency Interface Card (RFIC) for generating Y . Finally, the apparatus includes a gain unit for processing Y and W to obtain the final transmitted power Y .

Wheatley et al. in their patent disclosure describe a power control process that enables a mobile station to continuously update the base station on the power output required [19]. The authors explain a procedure for power control that the base station sends a frame to the mobile at a particular rate. If the mobile received and decoded the frame correctly, the mobile sets a power control bit in the next frame to be transmitted to

the base station. Based on the error rate of the received power control bits, the base station determines whether to increase or decrease the transmit power.

The other related patent is a disclosure that describes a method and apparatus for using multiple code rates for forward error correction in a cellular digital radio communication system. S. Gardner et al. disclose that each base station broadcasts a quantity called the power product (PP) that is equal to the base station transmit power, P_{BT} , multiplied by the power level received at the base station, P_{BR} [20]. In this model the mobile unit determines its appropriate transmit power, P_{MT} , by measuring its received power, P_{MR} . When the channel path loss is large, it is possible that the power control calculation will return a value greater than the maximum transmit power capability of the mobile unit. In such a case, the mobile unit selects a lower code rate. The base station receiver sensitivity improves as the code rate decreases, so the result is similar to increasing the transmit power. In the preferred embodiment, the invention uses three different code rates. In most cases, the code rate used is two-thirds. However, when a mobile unit determines that it needs more transmit power than it is capable of providing, the code rate is changed to one-half. In severe cases the code rate may be changed to one-third.

On the subject of rate change, a translated abstract from a Japanese patent, discloses reducing the Inter-Symbol Interference (ISI) at the time of demodulating signals from respective remote stations by preparing multiple chip rates and appropriately allocating them for the respective remote stations [21]. When the receiver determines that the maximum transmit power is not sufficient for error free transition, it selects a lower chip rate and signals the remote station of its new chip rate. In a remote station a

spreading code is generated corresponding to the chip rate informed from the base station.

In a summary, the prior art research and patent disclosures provide different algorithms and techniques for adaptive modulation including adaptive power control and dynamic rate changing. These techniques are mainly designed to reduce MAI and consequently aimed at increasing the channel capacity. However, due to the time variant nature of the mobile channels, inadequate adaptive closed-loop power control or rate change introduces the near-far effect and consequently increases the MAI. Therefore, a technique that can define an adaptive power and rate control policy for all users in a cell that can limit the MAI would be very valuable.

1.3 Problem Definition

Using as low transmitted energy as possible is the primary design goal for the developers of mobile systems. Strictly speaking, in wireless communications systems, this is important for increased battery life and reduction of interference. In an unbalanced and unmanaged system with an inadequate power control scheme, performance degradation and reduction in the channel capacity are vastly evident.

In conventional closed-loop power control, the ratio of the signal to interference plus noise is computed at the receiver and is compared with a set threshold value that is desirable for data transmission at a certain error probability. This technique suffers a large power penalty since most of the average signal power is used to compensate for deep fades where the base station receiver continuously requests for higher transmitter power from the mobile unit [22]. Consequently, the conventional algorithm for power

control ignores the fading channel characteristics in determining the optimum power control scheme.

Similarly, for the case of the multipath fading channels, where we include two, three or four paths, the same conventional power control scheme is applied to the transmitted symbols and no modification is made in this type of adaptive technique to optimize its performance. Consequently the traditional scheme would not perform ideally in this case. Furthermore, in the case of multi-user system, where each mobile system's transmit power is modified based on the individual receiver performance at the base station, there are no means to control and limit the average total transmit power of all users. Therefore, the inaccurate power management will increase the near-far effect at the base station receiver and significantly reduce system capacity.

1.4 Research Contribution

There are numerous constraints that determine when adaptive modulation may be used in a system. Typically, if the channel is changing faster than it can be estimated and the information is fed back to the transmitter, any adaptive modulation technique will perform poorly.

We propose a novel adaptive power control and rate change scheme for the W-CDMA system based on an algorithm for long-range prediction of the mobile channel for the fading channel proposed by Eyceoz et al. [23]. The authors of this paper find the linear Minimum Mean Squared Error (MMSE) estimate of the future flat fading coefficients given a number of previous observations. This algorithm characterizes the channel as an autoregressive model with lower channel sampling rate compared to the conventional data rate methods for fading estimations. The authors show that this

algorithm can reliably predict the future flat fading coefficients far beyond the coherence time of the fading channel.

Furthermore, we define a policy similar to the power control technique with thresholds with the exception that the thresholds in our Adaptive Transmitter Power Control (TPC) and Adaptive Seamless Rate Change (SRC) are set based on several regions of operation. These regions are defined by means of the probability distribution function (pdf) of the total average channel power. The pdf is initially constructed based on the history of the predicted channel power values derived from the long-range prediction algorithm. These regions can be defined such that the system operates at a constant average E_b/N_0 dictated by the policy.

The channel coefficients in the W-CDMA system can be recovered accurately at the receiver with the use of the pilot training symbols. Therefore, it is not necessary for us to predict the channel coefficients as explained previously [24]. However, in both the flat and the multipath-fading model, we instead exploit the long-range prediction of the total channel power. Furthermore, the power levels of each rake finger can be predicted and the strongest ones can be used in determining the optimum thresholds in our adaptive algorithm.

In a 1-user model with one channel path, the pdf of the channel power would be an exponential or chi-square function with 2 degrees of freedom. However, in a W-CDMA system, normally the rake receiver has several fingers. That is at the receiver, the system either estimates or predicts the channel coefficients at each rake finger and performs maximal ratio combining by multiplying each finger with its conjugate or

chooses the ones with the highest energy and performs maximal ratio combining on the selected fingers.

We present an example to further illustrate the performance of our proposed techniques in a multipath environment. In this example we choose a RAKE receiver with 4 fingers where each path corresponds to one of the RAKE fingers. If the receiver chooses only 2 of the highest power paths, which is using only 2 fingers out of 4, the total average channel power would be a combination of that for the two paths. In this case the pdf of the total channel power considering the 2 strongest paths is a chi-square function with 4 degrees of freedom. Consequently the thresholds for adjustment of Adaptive Transmitter Power Control (TPC) or Adaptive Seamless Rate Change (SRC) would be different from the previous case. One can generalize this by saying that for every path added into the system, the pdf of the total channel power becomes a chi-square with increments of 2 degrees of freedom.

Furthermore, in a two-user system where the multi-access interference is modeled as the Standard Gaussian Approximation (SGA), the system performance and error probability of our W-CDMA system becomes similar to the one for our one-user system. In this case the total noise power would be a combination of the thermal noise and the multi-access interference. Consequently, when all users adopt a similar policy for their adaptive power and rate control to our single user system in a flat or multipath-fading channel, the average total multi-access interference will be reduced. The resulting channel capacity of the system in this case will be increased and the system may operate in a lower transmit power level.

The organization of this research for the rest of the chapters is as follows. Chapter 2 discusses the characteristics of the mobile radio channel and the Rayleigh fading model in particular, and gives a brief overview of the channel prediction algorithm where we explain its application to our novel technique. Chapter 3 explains the system under study. We explain the Code Division Multiple Access techniques and the Wideband CDMA system. Chapter 4 is the core of the research and it describes the analytical results of the proposed adaptive technique for different channel environments. We also illustrate the performance of our proposed technique in the presence of other users. Chapter 5 describes the detailed simulation procedure and gives comparable results to the numerical calculations of chapter 4. The Conclusion is presented in chapter 6 of this Dissertation.

Chapter Two: Propagation, Characterization and Long Range Prediction of the Mobile Channel

2 Propagation, Characterization and Long Range Prediction of the Mobile Channel

Researchers have used two different approaches to investigate the nature of mobile radio channels. One approach is to try to get a comprehensive impression of the channel by its background in terms of physics. Another approach is to make numerous measurements of real channels to develop an empirical model. In either case we can only develop a model based upon statistical descriptions of the channel.

This chapter provides an overview of some existing channel models for wideband propagation from a theoretical point of view. The description of the channel models will be the basis for the derivation of the theoretical long-range channel prediction scheme and our proposed improved power and rate controlled techniques in the following chapters.

In a simple channel model, noise can be modeled as additive white Gaussian noise (AWGN) with zero mean and constant variance where it mainly stems from thermal noise in the amplifier. If there is no other distortion in the channel, this simple model is referred to as an AWGN channel.

This simple channel model is not always applicable. In a more general channel model, the signal is considered to be propagating over a multitude of paths. This model can be explained in terms of physics by the nature of the propagation paths with many independent scatterers. Therefore, a general channel model consists of a bandpass time variant filter that describes the channel disturbance followed by the addition of AWGN.

This model is shown in Figure 2.1. Here, $c(\mathbf{t},t)$ denotes the channel impulse response where \mathbf{t} is the time delay variable and t denotes the time dependence of the channel; $n(t)$ is the AWGN.

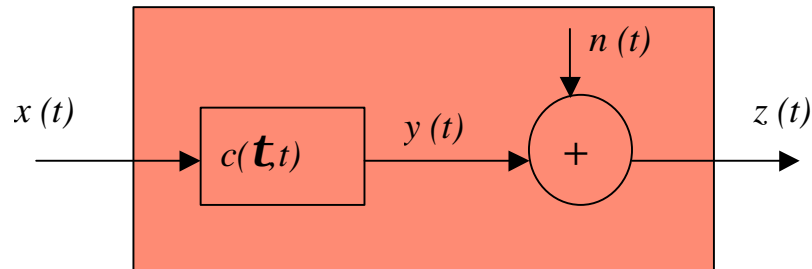


Figure 2.1. General Mobile Channel Model

Initially, in this model, the transmitted signal $x(t)$ is convolved with the channel impulse response, $c(\mathbf{t},t)$, and afterwards the white Gaussian noise, $n(t)$, is added to the signal. In the case of a pure AWGN channel as mentioned above, the channel impulse response is modeled as $c(\mathbf{t},t) = \delta(\mathbf{t})$.

2.1 Mobile Channel Characterization Functions

In order to describe the behavior of the mobile channel, we need to look at the functions that characterize the relationship between the input and the output of the channel both in the time and frequency domains [25,26].

Since the characteristic of the mobile channel impulse response in general is complicated and randomly distributed, the behavior of the channel must be described

statistically. Therefore, the autocorrelation function of the channel response is used instead of its impulse response to describe the mobile channel behavior.

$$\mathbf{f}_c(\mathbf{t}_1, \mathbf{t}_2; t_1, t_2) = \frac{1}{2} E[c^*(\mathbf{t}_1; t_1)c(\mathbf{t}_2; t_2)] \quad (2-1)$$

In many applications the channel is assumed to be Wide Sense Stationary Uncorrelated Scattering (WSSUS). The first property (WSS) of a stochastic process implies that the autocorrelation function depends on the time difference $\Delta t = t_2 - t_1$. The second property (US) states that the impulse response is independent at the two delays \mathbf{t}_1 and \mathbf{t}_2 due to the uncorrelated scatterers [27]. Therefore the autocorrelation function will look like,

$$\mathbf{f}_c(\mathbf{t}_1, \mathbf{t}_2; \Delta t) = \frac{1}{2} E[c^*(\mathbf{t}_1; t_1)c(\mathbf{t}_2; t_1 + \Delta t)] = \mathbf{f}_c(\mathbf{t}_1; \Delta t) \mathbf{d}(\mathbf{t}_1 - \mathbf{t}_2) \quad (2-2)$$

If we let $\Delta t = 0$ in (2-2), the resulting autocorrelation function $\mathbf{f}_c(\mathbf{t})$ explains the time delay behavior of the channel and provides a measure of the mean output power of the channel. This is called the *multipath intensity profile*. The multipath components of the transmitted signal that arrives at the receiver within a finite time duration becomes $\lim[\mathbf{f}_c(\mathbf{t})] = 0$ for $\mathbf{t} \gg T_c$. The time from when the first path arrives at the receiver until the time the last significant path signal arrives at the receiver is called the *delay spread* T_c of the channel. Figure 2.3 illustrates the multipath channel model with delay spread T_c .

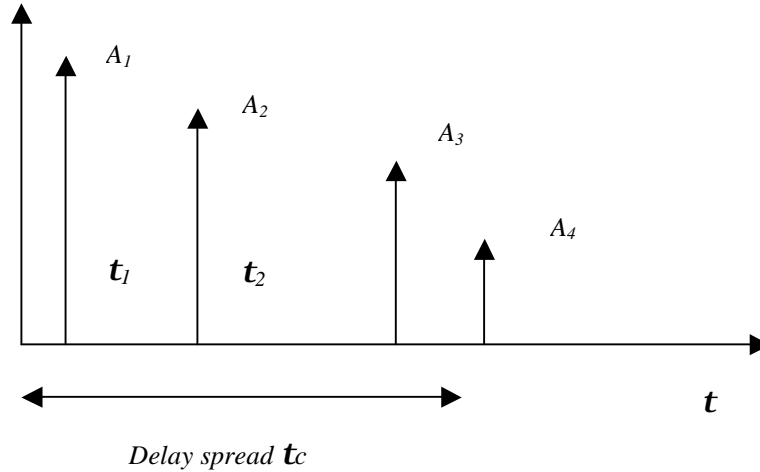


Figure 2.2. K-path Channel Model

We can apply the Fourier transform to $\mathbf{f}_c(\mathbf{t}_1, \mathbf{t}_2; \Delta t)$ with respect to the delay variables \mathbf{t}_1 and \mathbf{t}_2 to derive the *spaced-frequency spaced-time* correlation function. Let us once again set $\Delta t=0$ in this function to derive the function $\mathbf{f}_c(\Delta f)$ that provides information about the coherence of the channel in the frequency domain. We note that $\mathbf{f}_c(\Delta f)$ is the Fourier transform of $\mathbf{f}_c(\mathbf{t})$. Due to this relationship, the coherence bandwidth B_c of the channel is approximately the reciprocal of the delay spread T_c .

$$B_c \approx \frac{1}{T_c} \quad (2-3)$$

Both the coherence bandwidth and the delay spread serve for the characterization of the frequency selectivity in the mobile channel.

Let us once again consider the *spaced-frequency, spaced-time* correlation function $\mathbf{f}_c(\Delta f; \Delta t)$. Taking the Fourier transform of this function with respect to Δt results in the power spectral density $S_c(\Delta f; \nu)$ where ν is a frequency variable. Once again we set the parameter $\Delta f=0$ and we obtain the *Doppler power spectrum* $S_c(\nu)$ of the mobile channel [28]. The Doppler power spectrum gives a measurement of the frequency smearing that is the influence of the channel on the carrier frequency due to the Doppler effect and its effective bandwidth is referred to as the *Doppler Spread* B_d of the channel. We notice once again that $S_c(\nu)$ is the Fourier transform of $\mathbf{f}_c(\Delta f)$. Due to this relationship, we define the *coherence time* T_d of the channel, which is approximately the reciprocal of the Doppler Spread B_d .

$$B_d \approx \frac{1}{T_d} \quad (2-4)$$

The coherence time measures the duration of time that the channel is relatively constant. A slow moving channel has a large coherence time and consequently a narrow Doppler spread.

The last function to consider is the scattering function $S_c(\mathbf{t}; \nu)$ for the channel that can be represented as the Fourier transform of the autocorrelation function or the inverse Fourier transform of the power spectral density $S_c(\Delta f; \nu)$.

$$S(\mathbf{t}; \nu) = \int \mathbf{f}_c(\mathbf{t}; \Delta t) e^{-j2\pi\nu\Delta t} d\Delta t = \int S_c(\Delta f; \nu) e^{+j2\pi\mathbf{t}\Delta f} d\Delta f \quad (2-5)$$

We can illustrate a relationship between the channel parameters in a graphical representation.

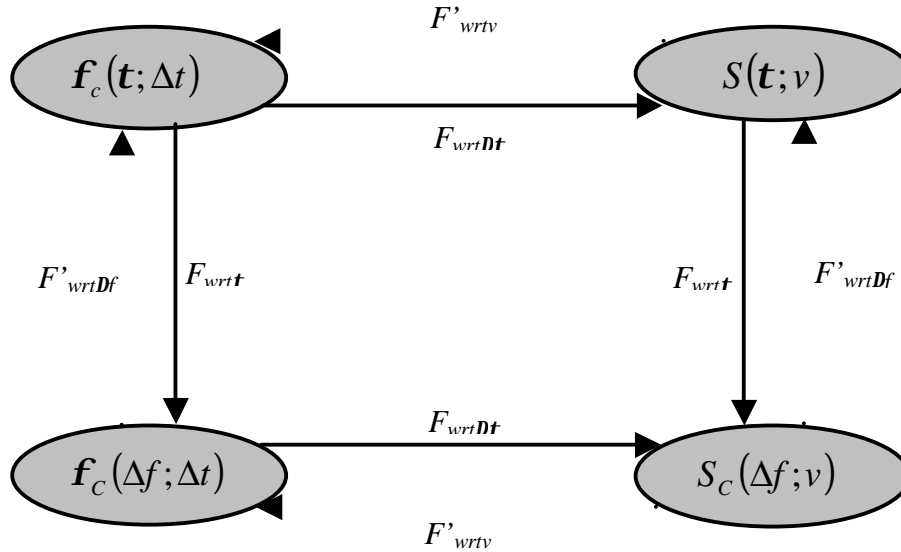


Figure 2.3. General Relationship between the Channel Characterization Functions

F , denotes forward and F' denotes inverse Fourier transform

2.2 Fading Channels

Fading is described as the fluctuation of the amplitude of the mobile signal in a short period of time. Fading is caused by the addition of two or more versions of the same transmitted signal arriving at the receiver at different times. The effect of multipath fading on the amplitude and the phase of the received signal depends on the propagation time, intensity, speed and the bandwidth of the signal.

An example for such a configuration is an outdoor channel environment as shown in Figure. 2-4. We note from this illustration that the signal propagates over several paths

while being affected by different physical phenomenon such as reflection, diffraction, and refraction. In this special example the receiver is moving away from the transmitter.

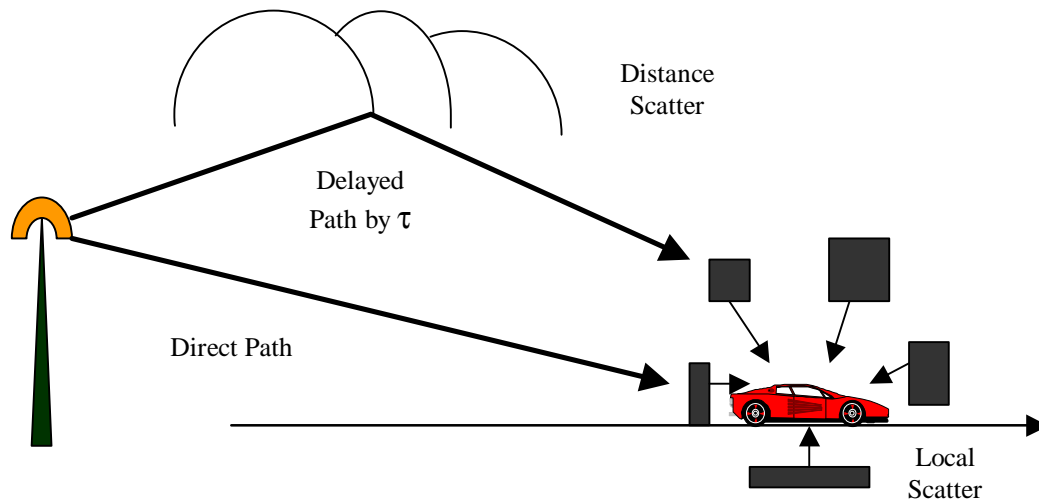


Figure 2.4. Typical Multipath Environment

In such channels, there are two concurrent effects that disturb the transmitted signal. The first one is the *frequency selectivity* due to multipath propagation and the second disturbance is referred to as *fading* due to the Doppler spread. We will describe these effects in great detail in this chapter.

2.2.1 Flat Fading Due to Delay Spread

If the response of the mobile channel has a constant gain and linear phase over a bandwidth that is greater than the bandwidth of the transmitted signal, the received signal will undergo *flat fading*. Figure 2.5 illustrates the characteristics of the flat fading channel.

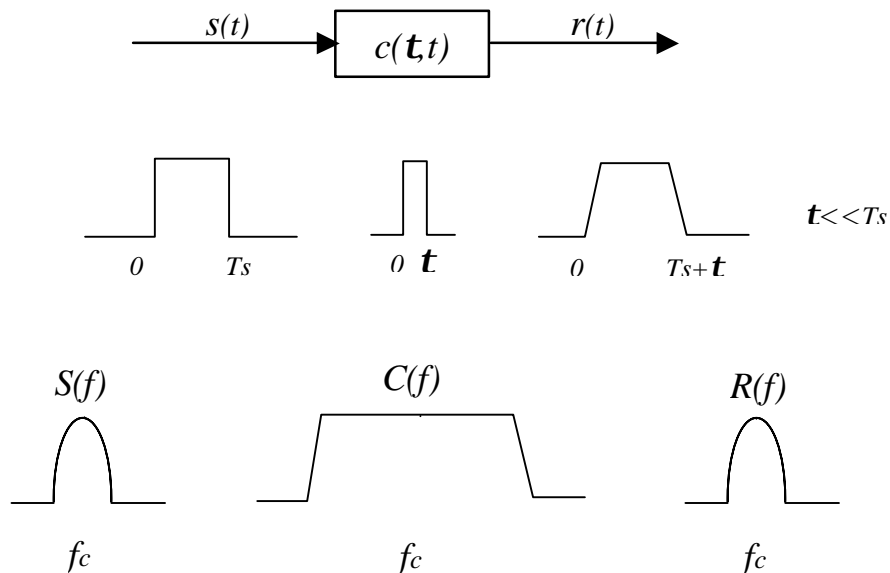


Figure 2.5. Flat Fading Channel Characteristics

We can see in Figure 2.5 that the signal $S(t)$ convolves with the narrow band channel coefficient $c(\mathbf{t}, t)$ and produces $r(t)$ that varies only in its gain. Therefore, flat fading channels are often called *amplitude varying channels* or *narrowband channels*. This is due to the fact that the bandwidth of the input signal is relatively narrow compared to the flat fading channel bandwidth. Typical flat fading channels cause deep fades that may require 20 to 30 dB more transmitter power to achieve a low Bit Error Rate (BER) compared to the system operating over a non-fading channel.

2.2.2 Frequency Selective Fading Due to Delay Spread

If a channel retains a constant gain and linear phase response over a bandwidth that is smaller than the bandwidth of the transmitted signal, the channel creates *frequency selective fading* on the received signal. In this case, the received signal contains multiple

instances of the transmitted waveform that are both attenuated and time delayed. These types of channels create inter-symbol interference (ISI) due to time dispersion of the transmitted symbols within the channel. In frequency selective fading channels, unlike Figure 2.5, the spectrum of the transmitted signal, $S(f)$, has a bandwidth that is greater than the coherence bandwidth B_C . The frequency selective fading channels are also known as wideband channels since the bandwidth of the signal $s(t)$ is wider than the bandwidth of the channel impulse response.

2.2.3 Slow and Fast Fading Due to Doppler Spread

Let us consider a mobile unit that is moving at a constant velocity v , along a path segment with length d , between points A and B. At the same time the mobile unit is receiving signals from a remote source S .

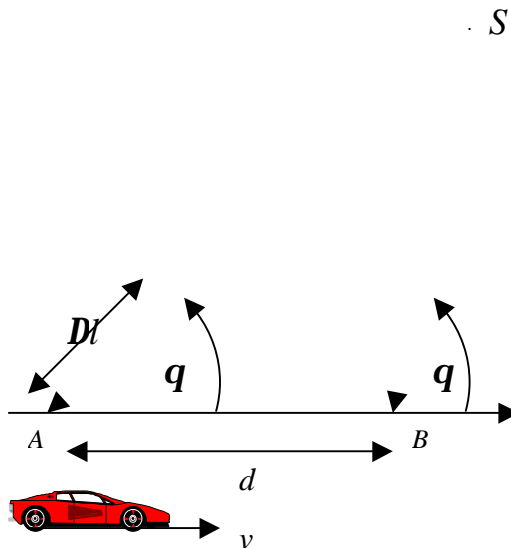


Figure 2.6. Doppler Effect

The difference in path lengths traveled by the waveform from the source to the point A and B is $\mathbf{Dl} = d \cos \mathbf{q} = v \mathbf{Dt} \cos \mathbf{q}$. In this equation, \mathbf{Dt} is the time that required for the mobile unit to travel from A to B and \mathbf{q} is the angle of arrival that is assumed to be the same for A and B. The change in the frequency or the Doppler shift is therefore given by

$$f_d = f_c \left(\frac{v}{c} \right) \cos \mathbf{q} \quad (2-6)$$

In the above equation, f_c is the carrier frequency, v is the velocity of the mobile unit, c is the speed of light and \mathbf{q} is the angle of arrival of signal to the mobile receiver. If the mobile unit moves in the direction of arrival of the signal, the Doppler shift is positive and if the mobile moves away from the direction of arrival of the signal, the Doppler shift is negative. Consequently, the multipath components from a continuous signal that arrives at the mobile unit from different directions contribute to Doppler spread and increase the signal bandwidth.

Depending on how fast the transmitted signal changes in comparison to the rate of change of the channel, the channel is considered a *fast or slow fading* channel. In a *fast fading* channel, the channel impulse response changes faster than the symbol duration. Therefore, the coherence time of the channel is smaller than the symbol period of the transmitted signal and then $T_s > T_c$. In a *slow fading* channel, the channel impulse response changes at a much slower rate than the signal. Therefore, the coherence time of the channel is much higher than the symbol period of the transmitted signal and then $T_s \ll T_c$.

In a W-CDMA system with a 5 MHz channel bandwidth, the received signal suffers smaller disturbance from fast fading effects. In outdoor environments, the deep fast fading suffered by channels with a bandwidth less than 1 MHz is about 30 dB, whereas the effect is much lower in a W-CDMA system [29].

2.3 Rayleigh Fading Model

In mobile communications, the statistical time varying nature of the channel envelope is normally described as Rayleigh distributed for both flat fading and for multipath fading for each individual path. In general, each path signal is assumed to be randomly distributed and mutually independent. The angle of incident for all signals is uniformly distributed and the signal paths are assumed to have the same mean power. Consequently, the resulting signal can be modeled as the superposition of a large number of complex random signals. The Rayleigh distribution is represented as the sum of the two-Quadrature Gaussian random processes due to the central limit theorem.

The W. Jakes model [30] and its slightly reformatted model [31] is a deterministic method for simulating the Rayleigh fading channels.

$$C(t) = \sum_{n=1}^N A_n e^{j(2\pi f_n t + \phi_n)} \quad (2-7)$$

The fading coefficients at the receiver BS are given by the above sum. In this case for the n^{th} scatter, A_n is the amplitude, f_n is the Doppler frequency, and ϕ_n is the phase. The complex Gaussian distribution of the Rayleigh-fading signal was modeled based on the assumption that the scattered signals are distributed uniformly around the mobile unit

over $[0, 2\pi]$ and the number of scatterers is infinity. It is also assumed that the parameters A_n , f_n and \mathbf{f}_n vary much slower than the actual fading coefficient $C(t)$. Figure 2.7 shows a Rayleigh distributed signal envelope as a function of the number of samples. The Doppler frequency is assumed to be at 200 Hz with a sampling rate of 4.096 MHz.

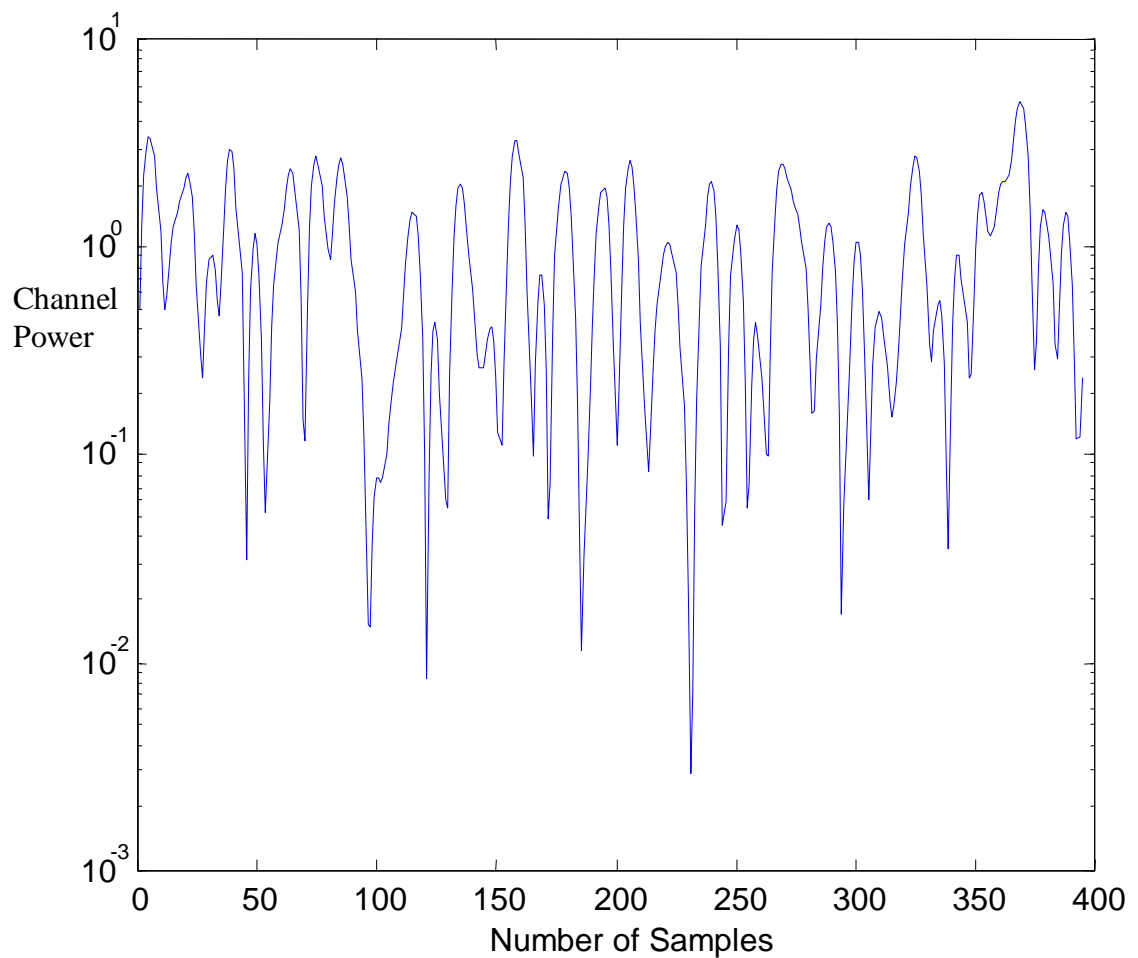


Figure 2.7. Rayleigh Fading Envelope at 4.096 Mcps

In mobile communication systems with high data rates, we need to model the effects of multipath delay spread as well as fading. Multipath is a common channel impairment that causes the reception of a sum of several delayed replicas of the transmitted signal. A commonly used multipath model is an independent Rayleigh fading 2-ray model [32]. The impulse response of a 2-ray fading channel model is given by the following equation

$$h(t) = C_1(t) + C_2(t - \tau) \quad (2-8)$$

Where $C_1(t)$ and $C_2(t)$ are independent Rayleigh distributed flat fading channel responses and τ is the time delay between the two rays.

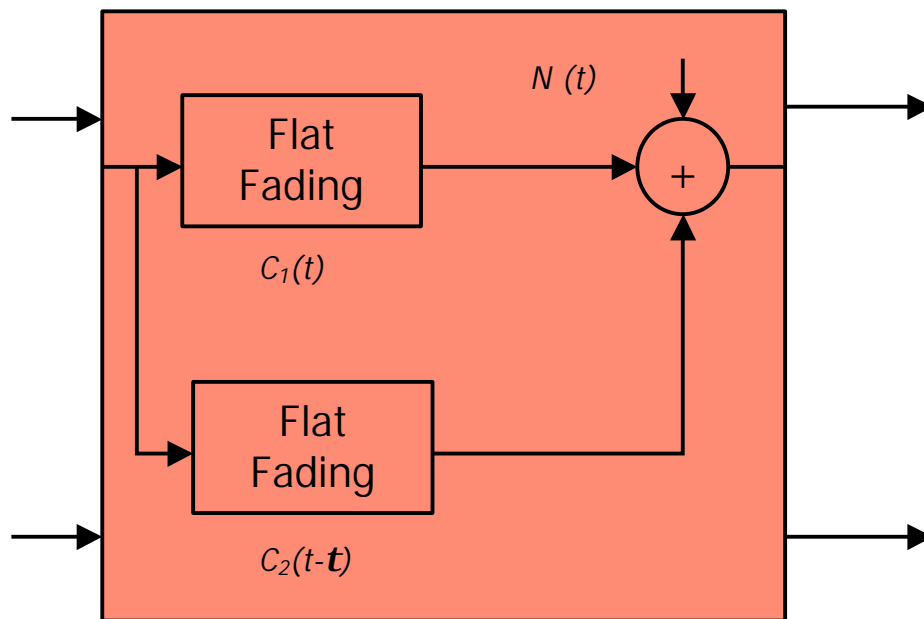


Figure 2.8. Two-Ray Multipath Channel Model

For our simulation results in the following chapters, we have used the two-path model as illustrated in Figure 2.8 where the transmitted signal is summed after being delayed and convolved with the two independent Rayleigh fading coefficients.

2.4 Long Range Channel Prediction

In a flat fading channel model, we can form the linear MMSE prediction of the future channel samples of $\hat{C}(t)$ in a discrete-time system based on the P previous channel samples that is determined as

$$\hat{C}_n = \sum_{j=1}^P d_j C_{n-j} \quad (2-9)$$

where the C_{n-1}, \dots, C_{n-p} are the previous channel samples that are sampled at least twice as fast as the channel Doppler frequency and the d_j 's are the linear prediction filter coefficients. The optimal coefficients d_j 's are computed as

$$\underline{d} = \underline{R}^{-1} \underline{r} \quad (2-10)$$

where $\underline{d} = (d_0 \dots d_{p-1})$, \underline{R} is the autocorrelation matrix ($p \times p$) with coefficients $R_{ij} = E[c_{-i} c_{-j}^*]$ and \underline{r} is the autocorrelation vector ($p \times 1$) with coefficients $r_j = E[c_{-j+n} c_{-j}^*]$.

Since the channel is modeled as the complex stationary Gaussian process, the corresponding autocorrelation function is given as

$$r(\underline{t}) = J_0(2\beta f_{dm} \underline{t}) \quad (2-11)$$

where $J_0(\cdot)$ is the zero-order Bessel function of the first kind.

In a realistic channel environment where the maximum Doppler frequency is around 200 Hz, the rate of the Doppler frequency is much lower than the sampling rate of the transmitted data at 4.096 MHz. Therefore, with a given order P , we can predict for much further in time than of the one step-ahead predictor. By adopting a recursive algorithm, channel parameters for several steps ahead can be predicted where the previously predicted samples are used for the observations of the future predicted samples [33]. This recursive algorithm also reduces the effect of the additive Gaussian noise encountered in the estimation of the channel coefficients.

In a frequency selective channel model with L paths, assuming each path is Independent and Identically Distributed (IID), there will be L predictive estimators similar to the flat fading that are operating at the receiver [34], and each has the form of (2-9). This investigation of the long-range prediction for the fading channel focuses on the case when the complex valued fading coefficients are predicted and observed. However, depending on the application, a different prediction problem may be of interest. For example, in the decision directed channel estimation, phase ambiguity requires differential encoding, and absolute phases are not available. This makes prediction of future phases problematic. But this is not a serious limitation, since implementation of many proposed adaptive coding methods depend on the knowledge of future power only, and phase prediction is not necessary. Thus, it is desirable to examine long-range prediction of the fading channel power using observed power samples.

2.5 Channel Power Prediction

In a system where pilot or training symbols are provided with every transmitted data slot, the coefficients of the fading channel can be accurately estimated at the receiver. These estimates can serve as the past observations where we compute the instantaneous predicted channel power for each path by

$$y_n = |\hat{C}_n|^2 \quad (2-12)$$

By substituting (2-12) instead of the channel coefficient into (2-9) we can form the linear MMSE prediction of the channel power such that

$$\hat{y}_n = \sum_{j=1}^P \underline{d}_j y_{n-j} \quad (2-13)$$

where the y_{n-1}, \dots, y_{n-p} are the previous instantaneous channel power samples that are sampled at a rate at least twice the channel Doppler frequency and the \underline{d}_j 's are the new linear prediction filter coefficients. The optimal coefficients \underline{d}_j 's are computed as

$$\underline{d} = \underline{R}^{-1} \underline{r} \quad (2-14)$$

where $\underline{d} = (d_0 \dots d_{p-1})$. \underline{R} is the autocorrelation matrix $(p \times p)$ with coefficients $R'_{ij} = E[y_{-i} y_{-j}^*]$ and \underline{r} is the autocorrelation vector $(p \times 1)$ with coefficients $r'_j = E[y_{-j+n} y_{-j}^*]$.

Furthermore, it can be easily shown that the corresponding autocorrelation function is given as

$$r'(t) = J_0^2(2\mathbf{p}_{dm}^f t) + N_0 J_0(2\mathbf{p}_{dm}^f t) + \frac{N_0^2}{2} \mathbf{d}(t) \quad (2-15)$$

Where $J_0(\cdot)$ is the zero-order Bessel function of the first kind and N_0 is the variance of the AWGN [35]. The resulting MMSE is given by the following equation.

$$E[|e_n|^2] = E\left[|y_n - \hat{y}_n|^2\right] = r'_0 - \sum_{j=1}^p d_j^- r'_j \quad (2-16)$$

In our simulations, we assumed a sampling rate of f_{dm} that is 1.6 KHz for our channel power prediction. Therefore in our channel model where we assumed a Doppler frequency of 200 Hz and Nyquist rate of 400 Hz, our selected channel prediction rate is 4 times higher than its Nyquist rate. Therefore, the predicted channel power would have a smaller MSE error compared to the case where it is operating at the minimum required sampling rate [33].

Chapter Three:

Multiple Access Technology

3 Multiple Access Technology

The wireless communications market is growing rapidly and the demand for higher system capacity and bandwidth is increasing. The analog cellular systems were designed 15-20 years ago when the demand was not as high as it is in today's market. Today's market demands large system capacity, low operations cost, revenue growth and finally smaller and friendlier user terminals. These features encourage the need for digital technology for wireless communications. There are basically three different technologies that share the spectrum resources for multiple users that can address the increasing demand of the wireless systems. These are Frequency-division Multiple Access (FDMA), Time-division Multiple Access (TDMA) and Code-division Multiple Access (CDMA).

3.1 Frequency Division Multiple Access (FDMA)

FDMA is a system where each user is assigned a different operating frequency for uplink and downlink. Guard bands are maintained between adjacent signals to minimize cross talk between users channel. The frequency bands are reserved separately for the uplink and down link [23,36]. These channels are assigned on demand to users who request service. During the period of the call, no other user can share the same frequency band. Each user is assigned a paired frequency in the channel. One is assigned for the downlink or forward channel while the other is used for the uplink or the reverse channel. This scheme is called Frequency Division Duplex (FDD). Figure 3.1 illustrates the FDMA system.

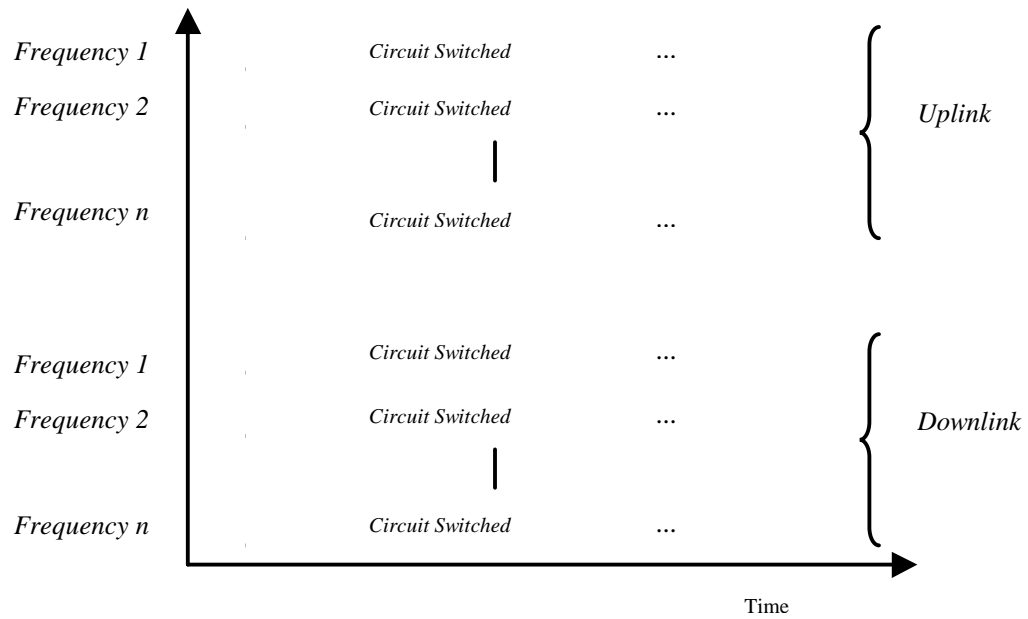


Figure 3.1. Graph of the Time Domain Vs Frequency Domain of the FDMA System

3.2 Time Division Multiple Access (TDMA)

The TDMA systems divide the radio spectrum into time slots and in each slot only one user is allowed to either transmit or receive in the Time Division Duplex (TDD) mode or transmitter and receiver simultaneously in the FDD mode. Each user, in this system, occupies a cyclically repeating time slot and each several time slots comprise a frame. In this system, data is transmitted in bursts and therefore the transmission for any user is not continuous. This implies that unlike the FDMA system where the transmission is continuous in each frequency band, the transmission in TDMA system is interlaced into repeating frame structure [37]. Figure 3.2 illustrates the TDMA system.

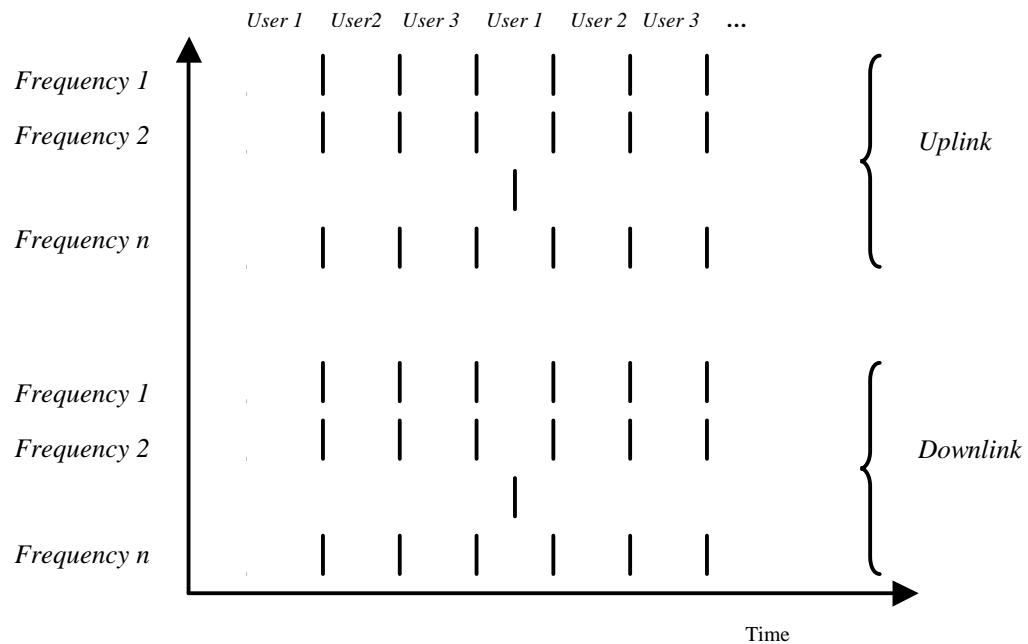


Figure 3.2. Graph of the Time Domain Vs Frequency Domain of the TDMA System

It can be seen from above that a frame consists of a number of slots. For the TDMA standard of IS-136 or formerly IS-54, the number of slots is specified as 3 per frame [38, 39]. In general the TDMA-FDD system intentionally induces several time slots of delay between the forward and reverse time slots of any user, so that duplicity is not necessary in the mobile unit. Similarly to the FDMA system, the bandwidth of each channel is relatively narrow, at 30 kHz. In the IS-54 standard however, each frequency band is shared between three users.

The capacity of the TDMA system, similarly to the FDMA system, is bandwidth limited. That is a predetermined number of channels are available for all mobile users. However, in comparison of the TDMA to the FDMA system, for each frequency channel, the capacity of the cellular system is increased by a factor of three times in the full rate

IS-54 standard system and six times as much in the half rate channel. The total number of channels is computed by multiplying the number of TDMA slots per channel by the number of available channels.

$$N = \frac{m(B_{tot} - 2B_{guard})}{B_c} \quad (3-1)$$

where m is the maximum number of TDMA users supported on each channel. There are two guard bands at the beginning and end of each frequency band to prevent interference from adjacent frequencies. From the above equation, we determine that the capacity of the TDMA system is similar to that for the FDMA system and is limited to the number of allocated frequencies and bands.

3.3 Code Division Multiple Access (CDMA)

In CDMA systems, the narrowband message signal is multiplied by a very large bandwidth signal called the spreading sequence. The spreading signal is a pseudorandom code sequence with chip rate that is an order of magnitude greater than the data rate of the message signal. All users in the CDMA system use the same carrier frequency and share the bandwidth. The data transmission may be done synchronously or asynchronously. Each user has its own pseudorandom codeword that is orthogonal to all other users.

The transmit power of users at the receiver determines the noise floor of the system after the correlation operation of the desired codeword with the received signal. If the power of each user within a cell is not controlled and the signals do not appear at

the receiver base station with the same power, the near far problem occurs. This problem is particularly severe in the direct sequence systems where multiple users operate at the same frequency band simultaneously with interference with one another [40]. Figure 3.3 illustrates the CDMA system where each channel is assigned a unique orthogonal pseudorandom code sequence.

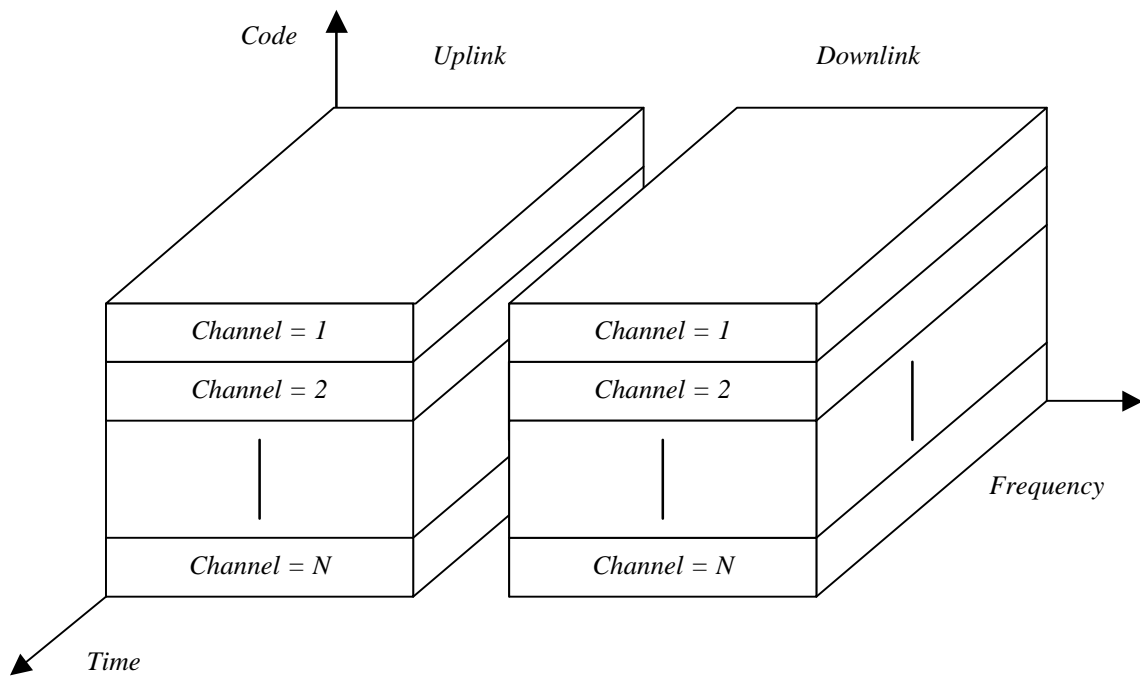


Figure 3.3. Graph of the Time Domain Vs Frequency Domain and Codeword of the CDMA System

In CDMA systems the stronger received signal level raises the noise floor at the base station for the weaker signals. Power control is used in CDMA system implementation to combat this problem. Each BS provides power control in a cellular system and if correctly applied, it assures that each mobile within the same coverage of the BS offers

the same signal power to the BS receiver. Power control is normally computed by rapidly sampling the signal strength at the receiver and comparing the estimated power level to a set known threshold and then sending power control commands to the transmitter over the forward channel. CDMA systems have several features. Some of these features are tabulated in the following table.

Table 3.1. CDMA System Features and Limitations

<i>Several users use the same frequency, TDD or FDD mode.</i>
<i>Unlike FDMA and TDMA, the CDMA system has soft capacity limits.</i>
<i>Multipath fading is reduced due to the spreading of the message signal.</i>
<i>The Channel data rate may be high due to the fact that the bandwidth is higher than FDMA or TDMA.</i>
<i>The Near-far problem limits the performance of the system if the power control scheme is not correctly applied.</i>
<i>Multi-access interference limits the performance of the CDMA system</i>

The second-generation CDMA cellular system is considered a narrowband CDMA system [41]. In the narrowband CDMA system the available wideband spectrum is divided into a number of small bandwidth spectrums. Each of these sub-channels forms a narrowband CDMA system where the processing gain is lower than that for the original

wideband CDMA system. Figure 3.4 illustrates the spectrum of the narrowband and the wideband CDMA system.

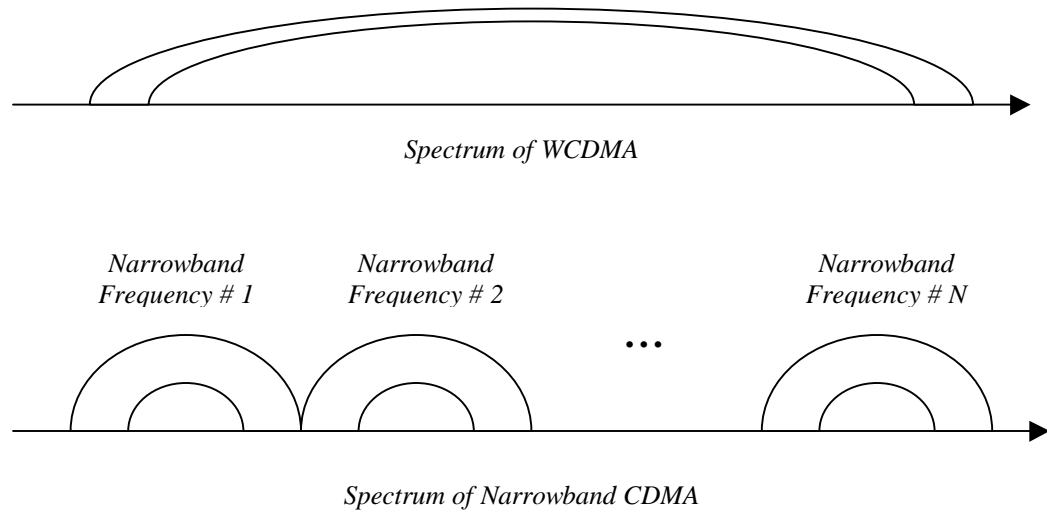


Figure 3.4. Spectrum of WCDMA Compared to the FCDMA

This type of system is called FDMA/CDMA or FCDMA system. The advantage of the FCDMA system is that different users can be allocated different bandwidths depending on their requirements.

3.4 Wideband CDMA System

Standardization of the third-generation mobile communication systems all over the world is rapidly in progress. Wideband CDMA has been chosen as the basic radio access technology in both Europe and Japan. In wide-band systems, the transmission bandwidth of a single channel is much larger than the coherence bandwidth of the channel. The WCDMA radio interface offers significant improvements such as increased coverage and

capacity due to a higher bandwidth compared to the second-generation narrow band CDMA system such as IS 95, where the available radio spectrum is divided into a large number of narrow-band channels. In W-CDMA, symbols are transmitted using Quadrature Phase Shift Keying (QPSK) and Direct Sequence CDMA (DS-SS-CDMA). Table 4.2, illustrates the key modulation parameters of the W-CDMA system.

Table 3.2. W-CDMA Modulation Parameters

Multiple Access Scheme	Wideband DS-SS-CDMA
Duplex Scheme	FDD
Chip Rate	4.096 Mcps (8.192 / 16.384 Mcps)
Carrier Spacing	4.4 – 5.0 MHz (200 KHz raster)

The basic chip rate is 4.096 Mcps, which is expected to expand to 8.192 and 16.384 Mcps in order to accommodate bit rates above 2 Mbps. W-CDMA uses the FDD scheme and has a flexible carrier spacing of 4.4-5.0 MHz with a carrier raster of 200 kHz. The 200 kHz carrier raster has been chosen to provide good coexistence and interoperability with the Global System for Mobile communications (GSM) network [42, 43].

3.4.1 W-CDMA Physical Channel Structure

W-CDMA defines two types of dedicated physical channels. One is the Dedicated Physical Data Channel (DPDCH) used to carry dedicated data generated at the layer 2 and above. The second is the Dedicated Physical Control Channel (DPCCH) that is used to carry layer 1 control information.

In the uplink, the DPDCH and DPCCH are coded and In-phase and Quadrature bits are multiplexed within each radio frame. The uplink DPDCH carries the control data while the DPCCH carries pilot bits, and Transmit Power Control (TPC) commands [44].

We can observe the channelization and scrambling of the uplink physical channel in Figure 3.5.

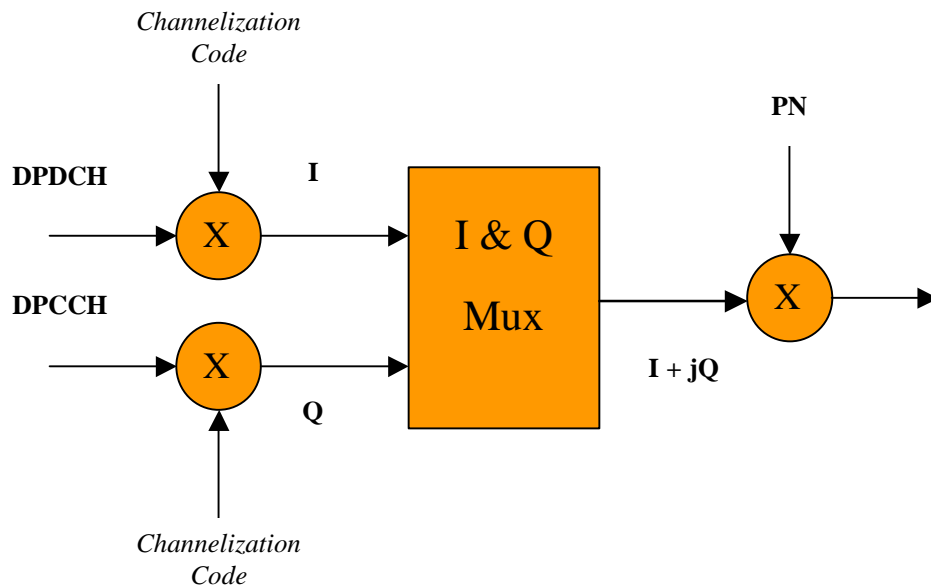


Figure 3.5. Uplink Channelization and Scrambling

In the basic operation, each physical channel is organized in a frame structure. Each frame of length 10 ms is divided into 16 slots of length 0.625 ms so that each slot consists of 2560 chips each corresponding to one power-control period. Therefore, the power-control and pilot symbol frequency is 1.6 kHz. For the downlink, pilot symbols are time-multiplexed with data symbols. That is every slot starts with a group of pilot symbols (4 or 8) that may be used to estimate or predict the channel and perform synchronization.

Figure 3.6 shows the uplink W-CDMA frame structure with the detail illustration of the DPDCH and DPCCH frames.

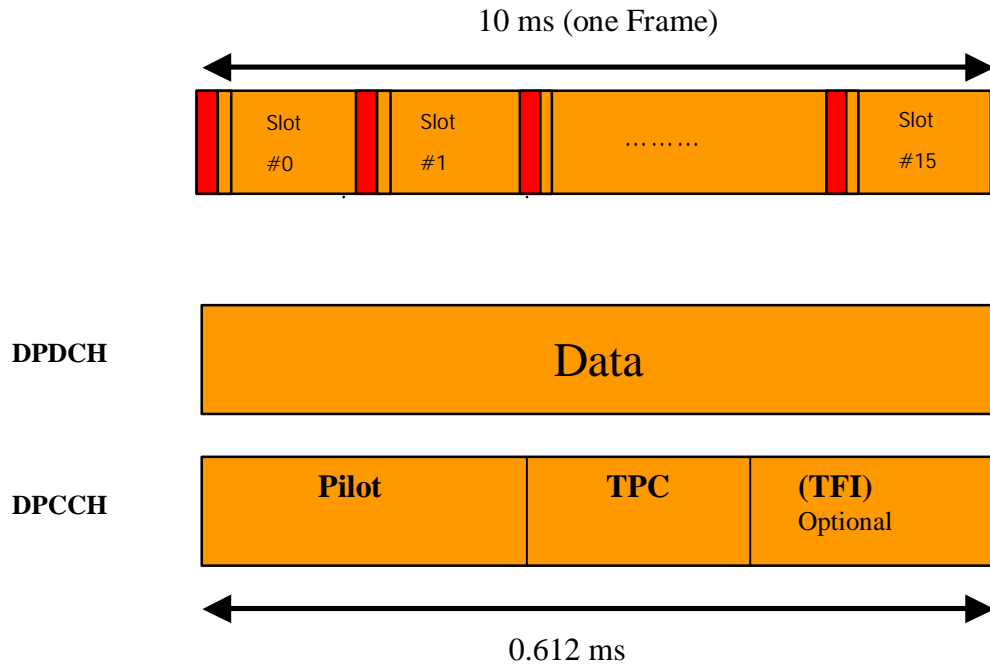


Figure 3.6. Uplink W-CDMA Frame Structure

3.4.2 Orthogonal Variable-Length Code

Improving the capacity of multimedia communications is one of the targets for W-CDMA mobile communications systems. W-CDMA is designed to support a variety of data services from voice to high-speed data and video. All users in the system have the same signal bandwidth and spread to the same chip rate. Therefore, multi-rate transmission requires multiple programmable Spreading Factors (SF).

Let each bit of the lowest bit-rate service be R_{min} and let it be spread by a code of length $N=2^n$, where $n = 1, 2, \dots, \log_2 R_{max}/2$. Also, let's assume another low bit-rate service is transmitting at $2xR_{min}$ where the bit duration is half that for the previous case. Then, we need a spreading code of length $N/2 = 2^{n-1}$ for spreading. In general a code length of 2^{n-k} is needed for bit rate $2^k R_{min}$. A method to obtain variable-length orthogonal codes that preserve orthogonality between users at different transmission bit-rates is presented in [45].

The Orthogonal Variable Spreading Factor (OVSF) code or the signature sequence is used to spread the data to the chip rate. The OVSF codes can be defined in a tree-like manner is illustrated in Figure 3.7.

Starting from $C_1(1) = 1$, a set of 2^k spreading codes with the length of 2^k chips are generated at the k^{th} layer. Generated codes of the same layer constitute a set of Walsh functions and they are orthogonal. In other words, a code can be selected in a system if and only if no other code on the path from the specific code to the root of the tree or the sub-tree is selected in the same BS [46].

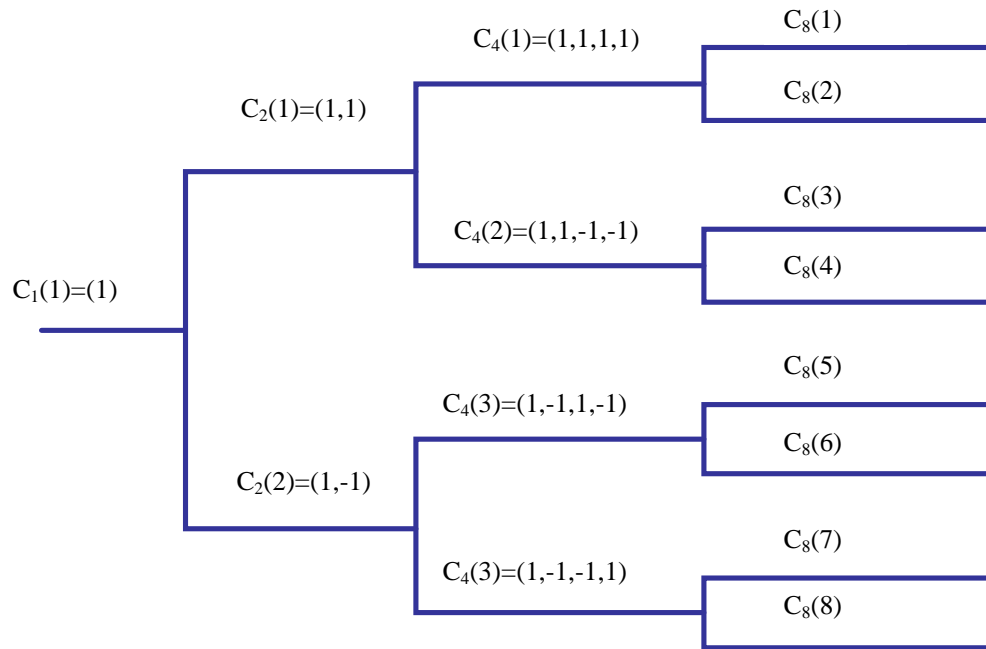


Figure 3.7. OVSF Code Tree

From this observation, we can easily find that if $C_8(1)$ is assigned to a user, all $\{C_{16}(1), C_{16}(2), C_{32}(1), \dots, C_{32}(4), C_{64}(1), \dots, C_{64}(8), C_{128}(1), \dots\}$ generated from this code cannot be assigned to other users requesting lower rates. The same provision applies for the mother codes that cannot be assigned to other users requesting higher rates. Therefore the total number of codes is not fixed. However it depends on the rate and spreading factor of each physical channel.

Smaller spreading factors are selected for higher transmit rates and larger spreading factors are used for the lower transmit rate. As noted in Figure 3.2, the two adjacent codes with the same parent are orthogonal. However, codes are not orthogonal to their own parents.

3.4.3 Multiple Spreading

A two layer spreading or multiple spreading code allocations provide flexible system deployment. As explained in section 2.1.1, orthogonality can be achieved by first multiplying each user's data by short spreading sequences which are orthogonal to one another in the same cell. This spread signal is followed by multiplication of a long pseudorandom noise sequence (PN) that is user specific in the cell. The short orthogonal codes are called channelization codes, and the long PN sequences are called scrambling codes. Each transmission channel code is distinguished by the combination of the channelization code and a scrambling code [47].

The uplink scrambling code can be either short or long. The short scrambling code is a complex code built of two 256-chip-long extended codes from VL-Kasami [48] set of length 255. The long scrambling code is a 40960-chips segment of a Gold code [49] of length $2^{41}-1$.

If the base station is using an advanced receiver structure such as interference cancellation multi-user detection, a short scrambling code is typically used for lowering the complexity of the receiver. When short codes are used, the cross-correlation properties are maintained between symbols, making the update of the cross-correlation matrix less complex. On the other hand in the cells where ordinary RAKE receivers are used, the long scrambling code is more appropriate.

3.4.4 Closed-Loop Power Control

The CDMA power control is a scheme to improve system performance and reduce multiple access interference. Reducing the short-term Rayleigh fading effect and

resolving the near far problem in the wireless reverse link may minimize the interference. The conventional fixed and variable step-size closed-loop power control has been proposed to combat this problem [50]. Although the fixed-size steps may not be adequate for a variable fading environment, the variable step-size power control also does not guarantee a constant power to be received at the base station. The threshold adjustment is typically based on the past behavior of the fading channel and the power control commands do not represent the current gain adjustment factor necessary to combat the variable fading effect [51, 52]. Figure 3.8 illustrates the power control structure.

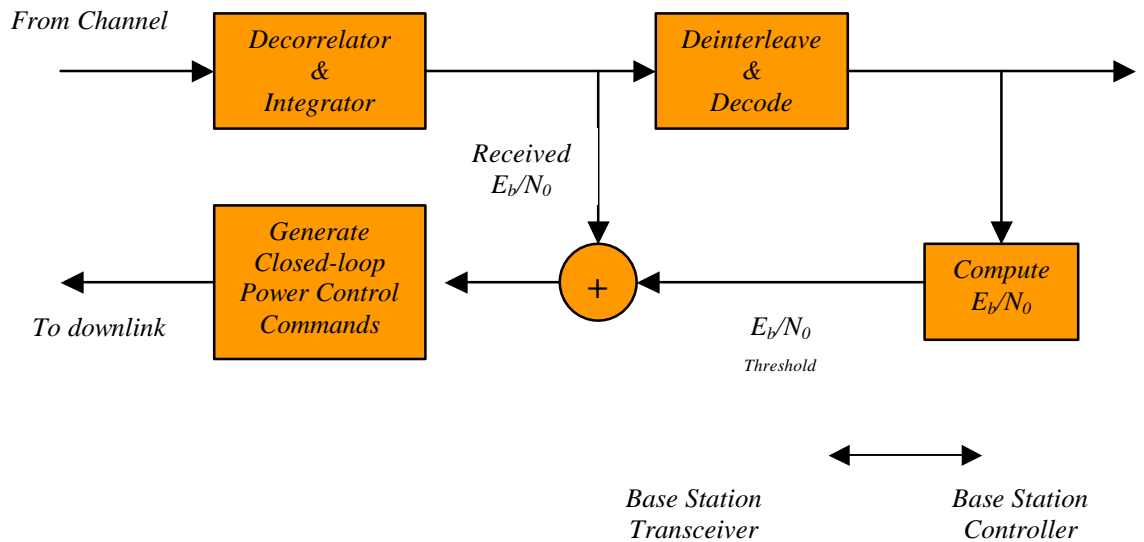


Figure 3.8. Closed-Loop Power Control Structure at the Base Station

The function of the power control system is such that the incoming signal is received from the channel and it is deinterleaved and decoded after the correlator bank of the rake

receiver. The received E_b/N_0 is compared to a threshold value and the commands are generated for the appropriate adjustment signal level for the mobile transmitter power control. These commands are sent to the mobile unit over the downlink transmission.

In a multi-user system, the goal of the BS is to manage the total transmitted power for all mobile users in a cell. However, the BS commands to each user must be such that the mobile station adjustment of its transmitted power is incremental and independent of all other user's adjustment. Consequently, the BS will not be able to minimize the multi-user interference of all users in the cell. Any improvement to the power control scheme that makes use of the statistics of the mobile channel to control the total interference is greatly beneficial in enhancing the capacity of the mobile system.

Furthermore, we propose a more efficient combination of a power and rate control scheme that minimizes the effect of MAI of a single user detector in a multi-user system. The following chapters describe the details of our powerful and novel technique.

Chapter Four:
Novel Adaptive Power and
Rate Control Techniques
with Analytical Results

4 Novel Adaptive Power and Rate Control Techniques with Analytical Results

Using as low transmitted energy as possible is a primary design goal in wireless systems where a reduction in transmitted power increases handset battery life and reduces intercell interference. In this regard, adaptive modulation is a very interesting topic that has attracted several researchers in the past [53, 54, 55, 56, 57]. These authors address more efficient and improved quality of service to the users by the use of several different adaptive modulation algorithms. Beside the system power management, system capacity and reliability are also of great importance in designing the next generation cellular system.

Our proposed schemes enhance the quality of the system by improved adaptive Transmitter Power Control (TPC) and adaptive Seamless Rate Change (SRC) with the objective of reducing the error probability while keeping the average transmit power constant. These techniques use the TPC bits and pilot symbols defined in the W-CDMA frame structure for signaling.

In mobile communication systems, the propagation channel is usually modeled as Rayleigh distributed [58] where the channel power has a chi-square probability distribution function with 2 degrees of freedom. Therefore the probability distribution function of the channel power $y = \alpha^2$ where α is complex channel coefficient and variance $E(y) = 2\sigma^2$ is

$$p(y) = \frac{1}{2\sigma^2} e^{-y/2\sigma^2} \quad (4-1)$$

The probability distribution function, γ_b , of the signal-to-noise ratio (SNR) at the receiver is

$$p(\mathbf{g}_b) = \frac{1}{\bar{\mathbf{g}}_b} e^{-\mathbf{g}_b / \bar{\mathbf{g}}_b} \quad (4-2)$$

$$\bar{\mathbf{g}}_b = \frac{\mathbf{e}_b}{N_0} E(\mathbf{a}^2) \quad (4-3)$$

where (4-3) is the average SNR at the receiver and the term $E(\mathbf{a}^2)$ is simply the average value of the channel power. In most W-CDMA systems, the channel has several multipath components. However, in this section, we concentrate on the flat fading case and later we discuss the case for the multipath-fading channel.

We apply the long-range channel prediction scheme presented in chapter 2 to implement our adaptive schemes. In our implementation, the BS for the next 10ms, or one future W-CDMA frame, predicts the future channel power. In our theoretical and simulation analysis, we assumed the BS prediction of the channel power at the beginning of each slot for the duration of a frame would be perfect, and the pdf of the predicted channel power is also chi-square with 2 degrees of freedom or exponentially distributed.

The modulation scheme applied in our derivations is antipodal BPSK signaling where a 0 bit is represented as a -1 and a 1 bit is represented as a $+1$. The probability of error for a BPSK is given by evaluating the integral,

$$P_2 = \int_0^{\infty} P_2(\mathbf{g}_b) p(\mathbf{g}_b) d\mathbf{g}_b \quad (4-4)$$

where

$$P_2(\mathbf{g}_b) = \frac{1}{2} \operatorname{erfc}(\sqrt{\mathbf{g}_b})$$

By substituting (4-2) into (4-4) and carrying out the integration for $P_2(\mathbf{g}_b)$, the resulting integral would become,

$$P_2 = \frac{1}{2} \left[1 - \sqrt{\frac{\mathbf{g}_b}{1 + \mathbf{g}_b}} \right] \quad (4-5)$$

Equation (4-5) is the closed form error probability for a BPSK system operating in a flat fading channel environment.

4.1 Adaptive Power and Rate Control

The traditional power control algorithms focus on controlling the interference by keeping the received power constant or performing Carrier-to-interference ration (CIR) balancing. This is normally achieved by reporting the past estimates of the power levels to the transmitter where the transmitter increases or decreases its power by a set increment.

Due to the random behavior of the mobile channel, when the traditional power control scheme is applied to the transmitted signal, most of the energy is used to combat the signals during the deep fades. Any increase in the transmitter power of one user causes an increase in the MAI on other mobile users. In this regard, by defining regions

of operations for each user of the mobile system, we can balance the MAI of each user and maintain a constant MAI.

However, the probability distribution function of the channel power for a Rayleigh fading channel is considered to be exponential or chi-squared distributed with two degrees of freedom. Consequently, to divide this pdf into several regions where the probability of every region becomes equal is not a trivial computation.

Furthermore, in a CDMA receiver, normally the rake receiver has several fingers due to the multipath signal arrival. That is at the receiver, the system either estimates or predicts the channel coefficients at each rake finger and performs maximal ratio combining by multiplying each finger with its conjugate or chooses the ones with the highest received energy and performs maximal ratio combining on the selected fingers by multiplying each finger output with the conjugate of the channel coefficients and combining the results.

In either case, the system performs the long-range power prediction of each finger to compute the total channel power. These values are used to modify the thresholds based on the new multipath channel power probability density function.

Figure 4.1 illustrates a three-region pdf of a Rayleigh distributed channel power.

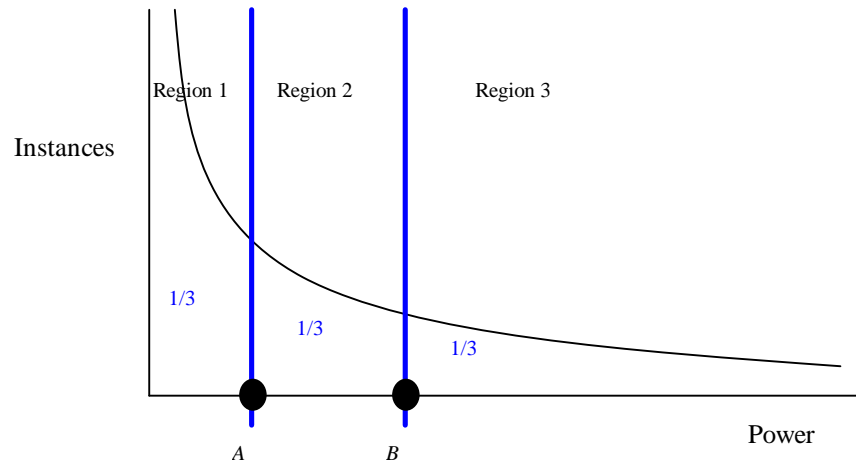


Figure 4.1. Three-Region pdf of the Channel Power

We can derive a three-region system as illustrated in figure 4.1 where the instantaneous predicted channel power value may fall in one of the three regions, $[0, A)$, $[A, B)$, or $[B, \infty)$ where the probability of each region is $1/3$. In other words, the probability that the system operates in poor, $[0, A)$, average, $[A, B)$, and high, $[B, \infty)$, channel conditions are the same. In this regard, we can define values “A” and “B” such that the above policy holds.

One could define an arbitrary number of regions of operation for our proposed scheme as long as the probability of all regions is equal. In the next chapter we define a 5-region and a 7-region of operation system where the probability of operating in each region is $1/5$ and $1/7$ respectively.

This policy allows the MS to configure its transmitter at the beginning of each W-CDMA time slot by modifying its power or adjusting its transmit rate based on a predetermined power adjustment level defined by the BS. This technique becomes possible to implement since the predicted channel power level at the beginning of every

transmitted slot is assumed to be available ahead of time at the MS transmitter. Therefore, the MS can compare the instantaneous predicted channel power level to the “A” and “B” values respectively and make appropriate adjustments to its transmitted information. In other words the MS can optimize its transmitter in order to minimize the probability of error at the BS receiver. We discuss this optimization in terms of TPC and SRC schemes.

4.2 General Procedure

We define a policy such that the MS transmitter modifies its transmitter power by multiplying its transmitted symbols by a gain factor or transmitter rate by a change in its spreading factor (SF) based on a threshold set by the BS. A channel probability distribution function is constructed initially based on the long-range prediction of the channel power. This PDF will be updated with the actual values derived from the channel estimation and instantaneous power calculations at the beginning of every W-CDMA slot. Next, thresholds will be set based on the constructed pdf so that the system operates 33% of the time in low-power region $[0, A)$, 33% of the time in the mid-power region $[A, B)$ and 33% of the time in the high-power region $[B, \infty)$.

4.2.1 Transmitter Power Control (TPC)

Implementation of the TPC technique is straightforward. When the instantaneous predicted channel power falls below the computed value of “A,” it implies that during the next data slot the system operates in a low channel power condition. Therefore the transmitter increases its transmitter power by a fixed value. In our analysis and simulation, we examine a 1-dB and a 3-dB increment policy for simplicity and further

comparison to the SRC technique. Similarly, when the instantaneous predicted channel power lies above the “B” value, the MS reduces its transmitter power by 3-dB. And finally, it makes no adjustment when the predicted channel power in the [A, B) region.

4.2.2 Seamless Rate Change (SRC)

The system can operate in the SRC mode to utilize the maximum capacity of the cellular system and reduce interference. In this case, if the predicted channel power falls below the “A” value, the MS reduces the transmit rate and it selects a predefined longer spreading code. In our simulation, two times the Spreading Factor (SF). When the predicted channel power goes above the “B” value, the MS increases its transmitter rate and selects a shorter spreading code, one half of the SF. Finally the system makes no adjustment to its transmitter and receiver when the predicted channel power lies in the [A, B) region.

In order to increase the capacity of the cellular system, the BS can make use of its available bandwidth and the SRC technique to signal the selected MS to reduce its transmitted rate. Reducing the transmitter rate is the same as increasing the processing gain, which allows the mobile user to reduce its transmitter power for achieving the same error probability at a lower rate. Consequently, reduction in the transmit power in an interference limited CDMA system increases the channel capacity which allows new users to be added into the system.

When the system chooses to increase or decrease the rate using its TPC bits, the BS signals the MS to modify its transmitted rate by halving or doubling the SF. For example if the nominal spreading factor is, “00111100,” the transmitter use code “0011”

for twice the rate and “0011110000111100” for half the rate transmission. Figure 4.2 illustrates the orthogonal code change for the SRC technique.

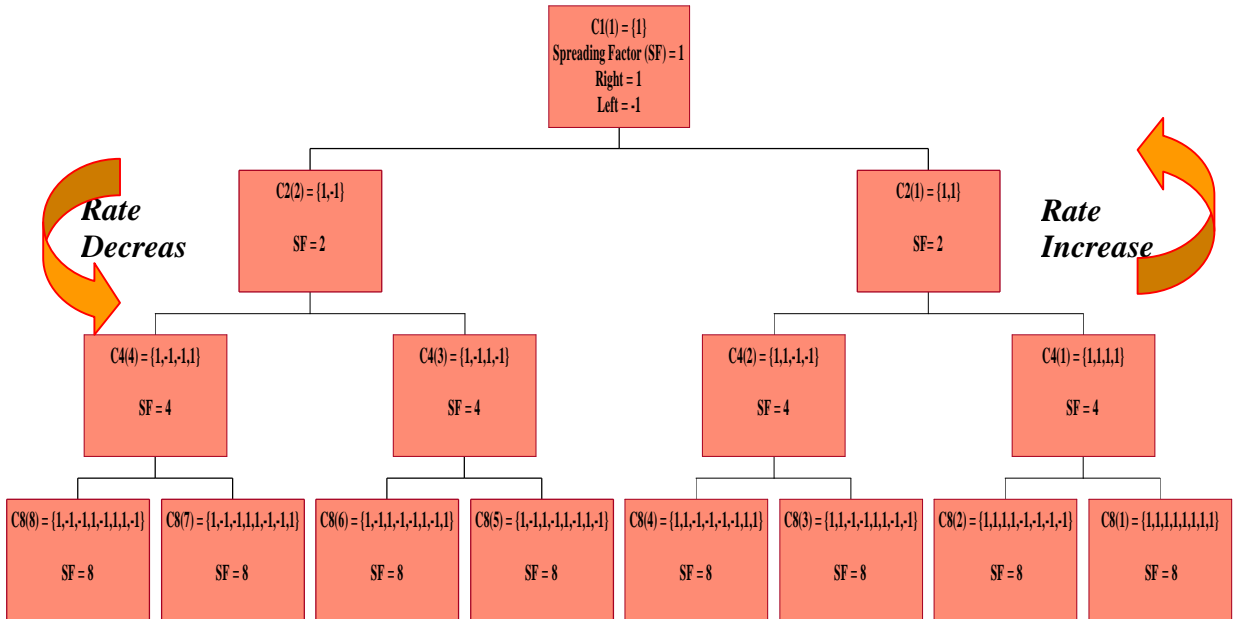


Figure 4.2. Orthogonal Code Change Scheme

SRC can also be used where there is excess bandwidth for the user to run its application. Since increasing the data rate by two has the same effect as doubling the transmitter power on the BER performance; SRC would be a better candidate to reduce BER where the system operates in a limited power consumption budget.

The MS transmitter and the BS receiver operate in a synchronous mode and adjust their transmitter or receiver according to a message sent by the pilot channel. The system can operate in a combination of the TPC, and SRC for optimum performance where excess bandwidth and power is available. For example, we can double the SF in conjunction with increasing the transmit power.

4.3 Analytical Results in Flat Rayleigh Fading Channel

Initially we assume the flat fading case. In our analytical work the average channel power is assumed to be equal to 1. Therefore, the average SNR (4-3) becomes,

$$\bar{g}_b = \frac{e_b}{N_0} \quad (4-6)$$

Therefore, in a system that operates in a three region TPC and the 3-dB adjustment policy, the transmitter would be operating at three distinct power levels at each region that the average SNR at the receiver become,

$$\bar{g}_{b_1} = 2\bar{g}_b \quad \bar{g}_{b_2} = \bar{g}_b \quad \bar{g}_{b_3} = 0.5\bar{g}_b \quad (4-7)$$

Where, 1, 2, and 3 are the indices corresponding to the three regions of the channel power pdf. Since the average channel power is assumed to be one, the above policy imposes a slight energy boost to the system when we apply a 1/3 probability.

$$\frac{1}{3}2\bar{g}_b + \frac{1}{3}\bar{g}_b + \frac{1}{3}0.5\bar{g}_b = x\bar{g}_b \quad (4-8)$$

where $x=1.1667$ is the gain value in our calculations. Therefore, to offset this power boost in our analysis, we have shifted the curves upward in the theoretical graphs and took the power amplification in account in our simulations.

The three different transmit power levels of (4-8) changes the probability distribution function of the received SNR at the receiver. Therefore, we can rewrite the pdf of (4-2) for the three different SNR values corresponding to each region.

$$p^n(\mathbf{g}) = \sum_{n=1}^M \frac{1}{\mathbf{g}_n} e^{-\mathbf{g}/\mathbf{g}_n} \quad (4-9)$$

In order to compute the thresholds for our adaptive modulation scheme, we need to initially integrate and evaluate (4-1) where $2\mathbf{s}^2=1$. In the low power region $[0, A)$ of the channel power pdf of Figure (4.1) we can compute threshold “A” by solving

$$\int_0^A e^{-y} dy = 1 - e^{-A} = \frac{1}{3} \quad (4-10)$$

where we can repeat (4-10) for the other regions $[A, B)$ and $[B, \infty)$, and calculate the other threshold “B” respectively.

By substituting (4-9) into (4-4), we determine the theoretical error probability of BPSK system operating at three transmit power regions to be,

$$P_2 = \int_0^{A.\bar{\mathbf{g}}} P_2(\mathbf{g}) p^1(\mathbf{g}) d\mathbf{g} + \int_{A.\bar{\mathbf{g}}}^{B.\bar{\mathbf{g}}} P_2(\mathbf{g}) p^2(\mathbf{g}) d\mathbf{g} + \int_{B.\bar{\mathbf{g}}}^{\infty} P_2(\mathbf{g}) p^3(\mathbf{g}) d\mathbf{g} \quad (4-11)$$

Where A , and B are normalized for each region with their corresponding SNR value for $p(\mathbf{g})$

It is not practical to compute a closed form equation for (4-11). Therefore, we used Mathematica [59], a numerical analysis tool, to solve the above equation in our analytical results. Numerical analysis tools normally solve complex equations by very close approximation methods. We have compared the results of the one region operation that produces the closed form (4-5) to the results solved by the numerical tool and the result perfectly match the results presented in text book reference [58]. Also since the simulation results closely match the closed form results and results computed by the numerical tool, we conclude that our theoretical results are accurate.

We computed the three integrals of (4-11) that correspond to the area under the curve of each region of the channel power pdf separately and sum the results for the total channel power. The result of each integral is the BER of the system when operated within the specified regions. Furthermore, when we define 5 and 7 regions of operation, the need to use a mathematical analysis tool such as Mathematica becomes more practical and necessary.

We can expand (4-11) for a multi-region TPC/SRC system and derive a general equation for our adaptive algorithm such as

$$P_2^N = \sum_{j=0}^{N-1} \int_{C_j \cdot \bar{\mathbf{g}}_{j+1}}^{C_{(j+1)} \cdot \bar{\mathbf{g}}_{j+1}} P_2(\mathbf{g}) p^{(j+1)}(\mathbf{g}) d\mathbf{g} \quad (4-12)$$

where N is the number of operation regions and the initial threshold value $C_0 = 0$, and the final threshold value $C_N = \infty$.

We calculated the theoretical error probability vs. energy per bit for a system with and without TPC/SRC for 3, 5 and 7 regions and a 1-dB adjustment policy and illustrated the results in Figure 4.3.

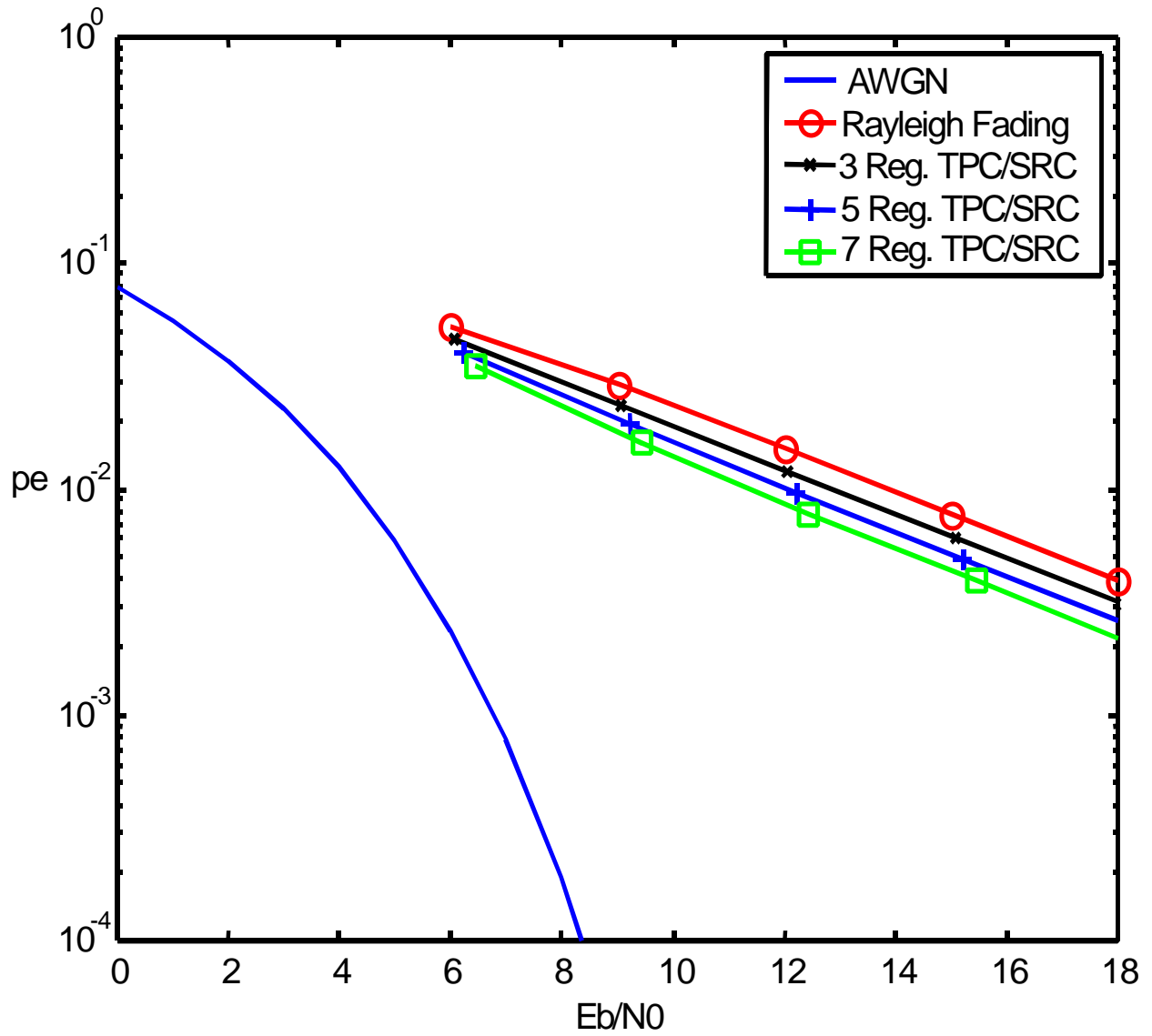


Figure 4.3. Theoretical P_e vs. E_b/N_0 with/without TPC/SRC 1-dB Adjustment

A 1-dB increment in the power control scheme, where it is a small adjustment in the power control technique, reduces the probability of error of the system in smaller increments. Consequently the system may not be utilizing its optimum performance.

Figure 4.4 shows the theoretical performance of the uncoded system with a 3-dB adjustment policy.

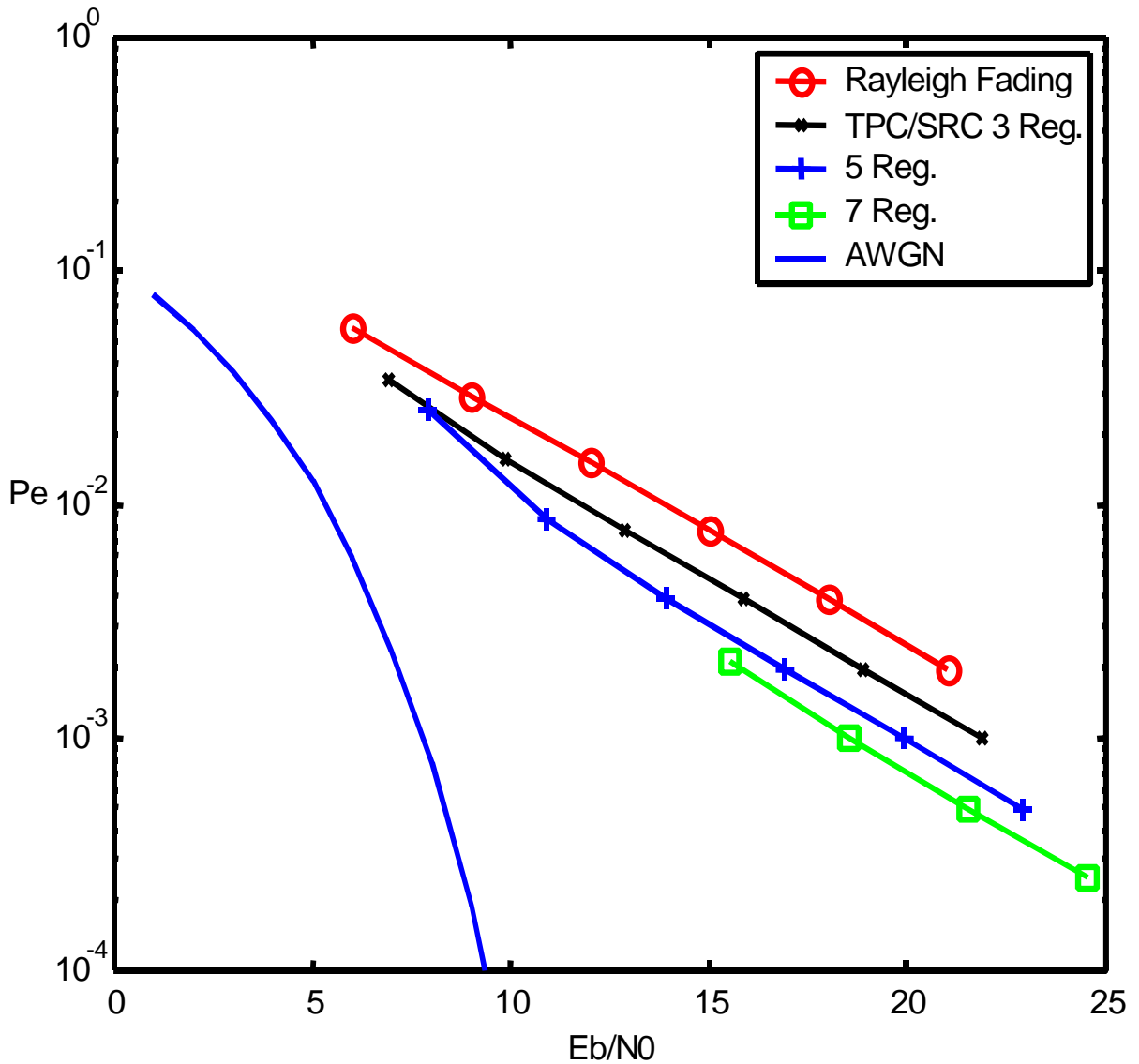


Figure 4.4. Theoretical P_e vs. E_b/N_0 with and without TPC/SRC with 3-dB Adjustment

Figure 4.4 illustrates the error probability of our proposed scheme as compared to the Rayleigh-fading channel with no power or rate adjustment and the AWGN channel. A 3-dB power adjustment is also represented as doubling or halving the data rate in the SRC scheme.

The top curve in Figure 4.4 illustrates the performance of a BPSK system with no adaptive power or rate control. The bottom curve is the reference AWGN channel that is the system upper bound performance. The three middle curves illustrate the performance of the BPSK system in conjunction with our proposed power control scheme

It is clear from the graph that the performance of our TPC or SRC techniques improves as the number of regions increments. The improvement for increasing the number of regions decreases as the number of regions increase. Since doubling the transmit power of each bit has the same effect as using twice as long a code sequence for each symbol, the theoretical values of the uncoded error probability for TPC and SRC are the same.

4.4 Analytical Results in Multipath Rayleigh Fading Channel

Let assume we have a rake receiver with 4 fingers with each multipath corresponding to one of the finger. After performing the long-range prediction for each path, if the receiver chooses to use only 2 of the highest power paths, the total average channel power would be a combination of that for the two paths. In other words the receiver is using 2 fingers out of the 4 such that,

$$Y(n) = \sum_{i=1}^L |C_i(n)|^2 \quad L=2 \quad (4-13)$$

In this case the pdf of the total channel power considering the 2 strongest paths is a chi-square function with 4 degrees of freedom. Consequently the thresholds for adjustment of the adaptive transmitter power control would be different from the previous case. One can generalize this by saying that for every path added into the system, the pdf of the total channel power will be varied and it becomes a chi-square pdf with $n=2,4,6\dots$ degrees of freedom such that,

$$p(y) = \frac{1}{2^{n/2} \mathbf{s}^n \Gamma(n/2)} y^{(n/2)-1} e^{-y/2\mathbf{s}^2} \quad (4-14)$$

where $\Gamma(q) = (q-1)!$ is the Gamma function and n is the degrees of freedom.

Figure 4.5 illustrates the pdf of the predicted channel power for $L=1, 2, 3,$ and 4 path Rayleigh fading channels with $2L$ degrees of freedom. In this plot we see that as the number of the paths increases, the distribution of the channel power becomes closer to a Gaussian distribution due to the fact that the sum of large number of Independent Identically Distributed (IID) random variables approaches a Gaussian distribution [60].

The sampling rate to compute the channel powers pdf of Figure 4.5 is the same rate as the sampling rate of the pilot symbols in the W-CDMA slots. These channel power values are computed from the channel coefficients that are recovered adaptively at the beginning of each slot. As noted in previous chapters, a 10 ms W-CDMA frame is divided into 16 slots of 0.626 ms.. At the beginning of each slot there are several symbols of pilot or training sequences that are used to recover the channel coefficients.

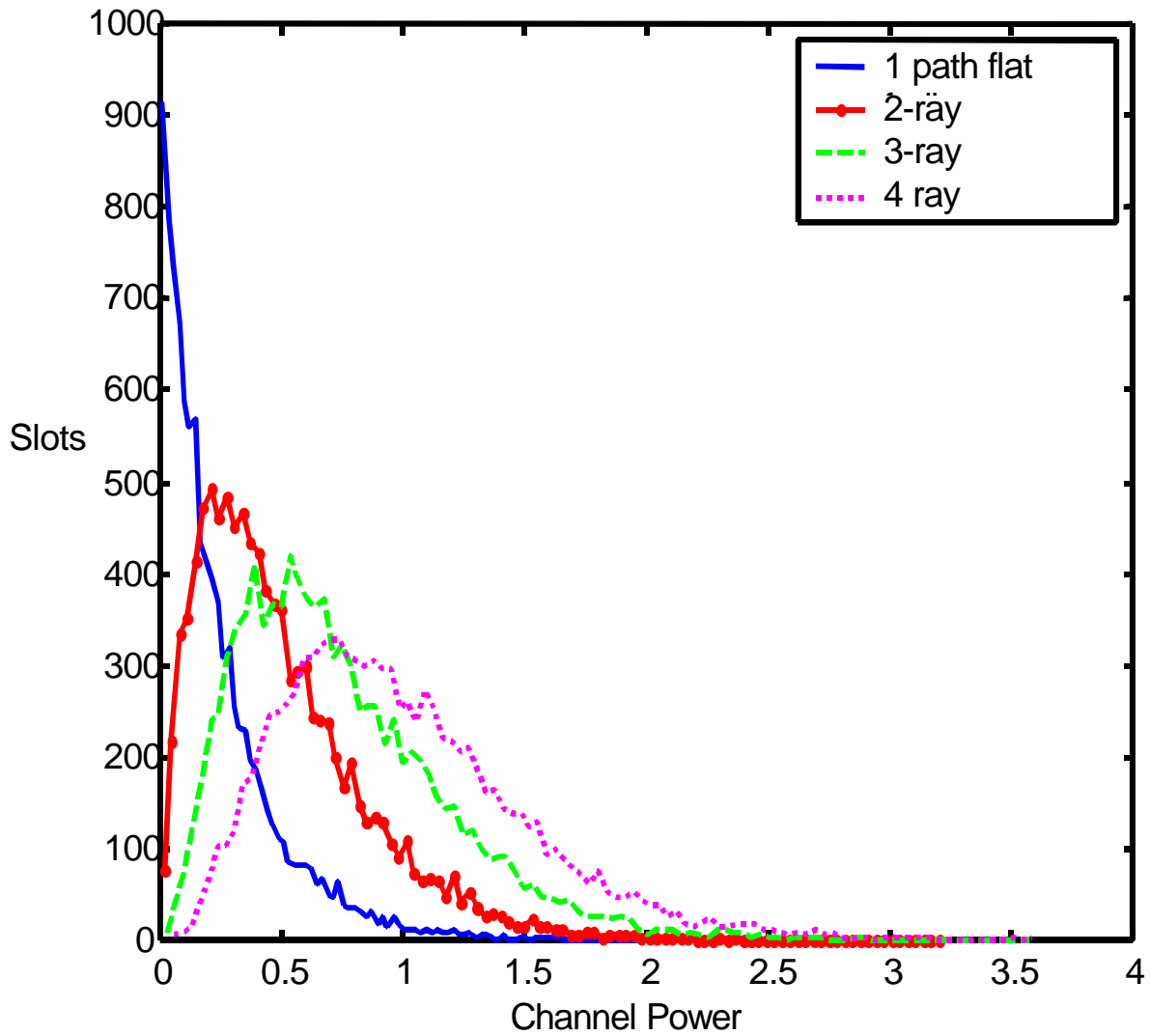


Figure 4.5. Channel Power pdf for 1, 2, 3 and 4 Paths

It is clear from Figure 4.5 that if we were dividing the multipath channel power pdf into three, five or seven regions, the thresholds for the new segments would become a different value for 1, 2, 3, or 4 paths. This graph is obtained from actual simulation of the W-CDMA system where for each path the fading coefficients are assumed to be independent.

Consequently the new $\bar{\mathbf{g}}$, which is the new average SNR at the receiver for the multipath case becomes

$$\bar{\mathbf{g}} = \frac{e_b}{N_0} \sum_{k=1}^L [E(\mathbf{a}_k^2)] \quad (4-15)$$

Similarly to the flat fading case, the total average channel power in (4-15) is normalized to one.

Similarly, in a system using TPC and the 3-dB adjustment policy, the transmitter operates at three transmit levels and consequently the average SNR at the receiver becomes the same as given in (4-15). The pdf of the average SNR at the receiver for a chi-square-distributed random variable with $2L$ degrees of freedom where L is the number of paths is given by

$$p(\mathbf{g}) = \frac{1}{(L-1)! \bar{\mathbf{g}}^L} \mathbf{g}^{L-1} e^{-\mathbf{g}/\bar{\mathbf{g}}} \quad (4-16)$$

By substituting (4-16) into (4-4) where the system operates in one region, we can compute the closed form error probability for a BPSK system operating in a multipath fading channel environment as

$$P_2 = \left(\frac{1-\mathbf{m}}{2}\right)^L \sum_{k=0}^{L-1} \binom{L-1+k}{k} \left(\frac{1+\mathbf{m}}{2}\right)^k \quad (4-17)$$

$$\text{where, } \mathbf{m} = \sqrt{\frac{\bar{\mathbf{g}}}{1+\bar{\mathbf{g}}}}$$

If we adopt the three-region TPC/SRC for power management, the new pdf for the received SNR in multipath fading channel becomes

$$p^n(\mathbf{g}) = \sum_{n=1}^M \frac{1}{(L-1)! \mathbf{g}_n^L} \mathbf{g}^{L-1} e^{-\mathbf{g}/\bar{\mathbf{g}}_n} \quad (4-18)$$

where $n=1, 2, 3, \dots$, is the operating region number and not the power.

The theoretical error probability of a BPSK system operating at three transmit power regions will become similar to (4-11) where we need to integrate and evaluate (4-15) for the three regions, and solve for the new thresholds A_l and B_l similar to (4-10). Therefore the exact equation for the probability of error will become once again (4-19) where the lower and upper thresholds are normalized with the corresponding SNR values and (4-18) replaces (4-9).

$$P_2 = \int_0^{A_1 \cdot \bar{\mathbf{g}}} P_2(\mathbf{g}) p^1(\mathbf{g}) d\mathbf{g} + \int_{A_1 \cdot \bar{\mathbf{g}}}^{B_1 \cdot \bar{\mathbf{g}}} P_2(\mathbf{g}) p^2(\mathbf{g}) d\mathbf{g} + \int_{B_1 \cdot \bar{\mathbf{g}}}^{\infty} P_2(\mathbf{g}) p^3(\mathbf{g}) d\mathbf{g} \quad (4-19)$$

In the above equation, A_l , and B_l are normalized for each region with their corresponding SNR value for $p(\mathbf{g})$. Similarly to the case for (4-11), a closed form equation for (4-19) is not practical. Therefore we applied Mathematica software to solve the complicated integral through approximation. We compared the results of the one region operation that produces the closed form (4-17) to the results solved by the numerical analysis tool and the result perfectly match the result presented in the textbook reference [58].

The calculated theoretical error probability vs. energy per bit for a system with and without TPC or SRC for 1, 2 and 4-path Rayleigh fading channels operated at different numbers of regions are plotted in Figure 4.6.

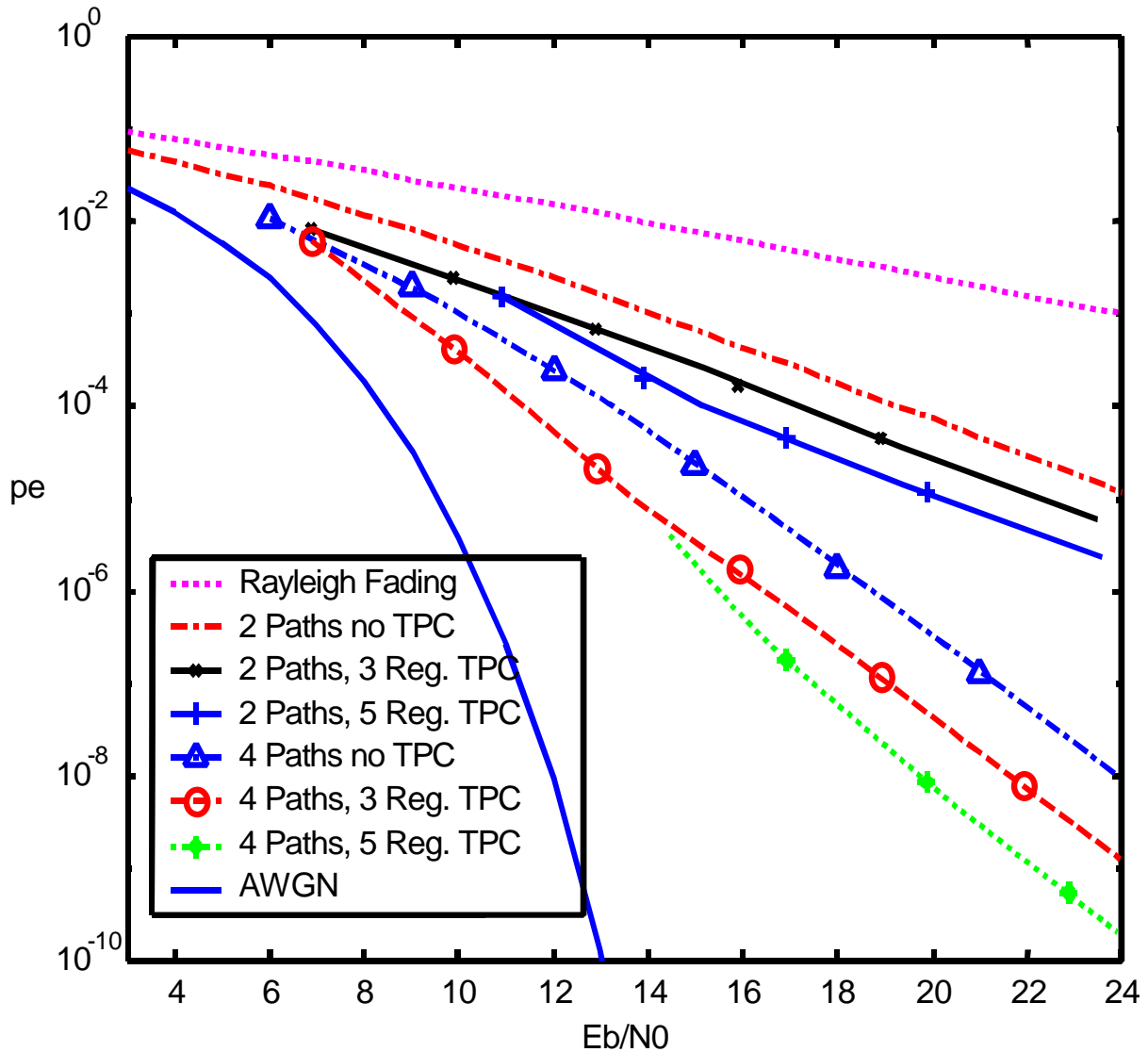


Figure 4.6. Theoretical Pe vs. Eb/N0 with/without TPC/SRC, 1, 2, & 4 Paths

It is clear from Figure 4.6 that the theoretical performance of the uncoded system as compared to the Rayleigh-fading and the multipath fading is superior. It can also be

noted from the graph that the performance of the TPC and SRC systems improve as the number of transmission paths increases and also as the number of region increments increases. Similarly to the case for flat fading, the improvement for increasing the number of regions decreases as the number of regions increase.

4.5 Analytical Results for Multi-user Performance

Let us initially look at a basic CDMA system with K -users. This system consists of the sum of antipodal modulated synchronous signature codes in an Additive White Gaussian Noise (AWGN) channel. Secondly, we introduce the Rayleigh fading channels to examine the performance of our proposed system in a multi-user channel model. In this case the received signal would become

$$y(t) = \sum_{k=1}^K A_k b_k s_k(t) + n(t) \quad t \in [0, T] \quad (4-20)$$

where T is the inverse of the data rate, and $s_k(t)$ is the known orthogonal variable spreading sequence for user k and is normalized such that

$$\|s_k\|^2 = \int_0^T s_k(t) dt = 1 \quad (4-21)$$

A_k is the received amplitude and the b_k is the transmitted bits for the k^{th} user. Finally $n(t)$ is the AWGN that models the thermal noise and other sources of unrelated signals that can be modeled as WGN [61].

For most practical applications such as the mobile handset, single user detectors are considered to be a better candidate for implementation in the hardware. The conventional matched filter detector consists of a single-user-matched filter that is matched to the signature code of the user of interest. Therefore detection is also based on the output of the filter for the user of interest. It is known that the performance of the single user detector suffers from the near-far problem. That is the weakly received or far user's signal may be corrupted by the strong or near user's signal. Therefore, optimum and sub-optimum single and multi user detectors have been developed to combat this problem [62, 63, 64]. Due to the high complexity of the multi-user detectors, these classes of detectors are strong candidates for BS receivers and not for MS receivers.

Consider K users transmitting synchronously using binary CDMA over a Rayleigh fading frequency non-selective channel. At the receiver, there are K matched filters that de-spread each user's signal. In discrete time, we can write the output of the correlator bank in the baseband as

$$y_k(1) = C_k b_k \sum_{j=1, j \neq k}^K r_{kj} C_j b_j + n_k \quad k = 1, \dots, K \quad (4-22)$$

where C_k are IID zero-mean complex Gaussian fading coefficients, and b_k and n_k are data bits and AWGN. The normalized cross correlation between the two signature waveforms of user l and user K is r_{kj} for $j=1$. If the signature waveforms are orthogonal, the cross correlation r_{kj} becomes zero and the Multiple Access Interference term

disappears. Therefore, the matched filter output (4-22) reduces to a single-user problem where

$$y_k = C_k b_k + n_k \quad (4-23)$$

In this case the probability of error for such a system would become the same as (4-5) which is the same error probability we obtain in the absence of other users. Since the presence of other users cannot reduce the probability of error, the bank of single-user-matched filters is only optimum in the synchronous orthogonal CDMA case. Due to the effect of fading, the r_{kj} is not zero where in this case the system under study becomes a non-orthogonal CDMA. In a k-user system [62], the exact BER expression for user 1 with a single-user detector in a flat Rayleigh fading channel and AWGN is similar to (4-5) that is given by

$$P_2 = \frac{1}{2} \left[1 - \sqrt{\frac{\bar{g}_{eq}}{1 + \bar{g}_{eq}}} \right] \quad (4-24)$$

where the equivalent SNR for the above BER is

$$\bar{g}_{eq} = \frac{\xi_1}{1 + \sum_{j=2}^K (r_{1j})^2 \bar{g}_j} \quad (4-25)$$

In these calculations no approximation is used. For non-orthogonal CDMA where the signature sequences are not deterministic, the correlation between the two signature waveforms of user l and user K becomes

$$r_{1j} = \frac{1}{N} \sum_{l=1}^N s_{1l} s_{jl} \quad (4-26)$$

In this case the variance of r_{1j} evaluates to $\frac{1}{N}$ where we can replace $(r_{1j})^2$ with $\frac{1}{N}$ in (4-25) and N is the spreading factor [65]. Figure 4.7 illustrates this approximation

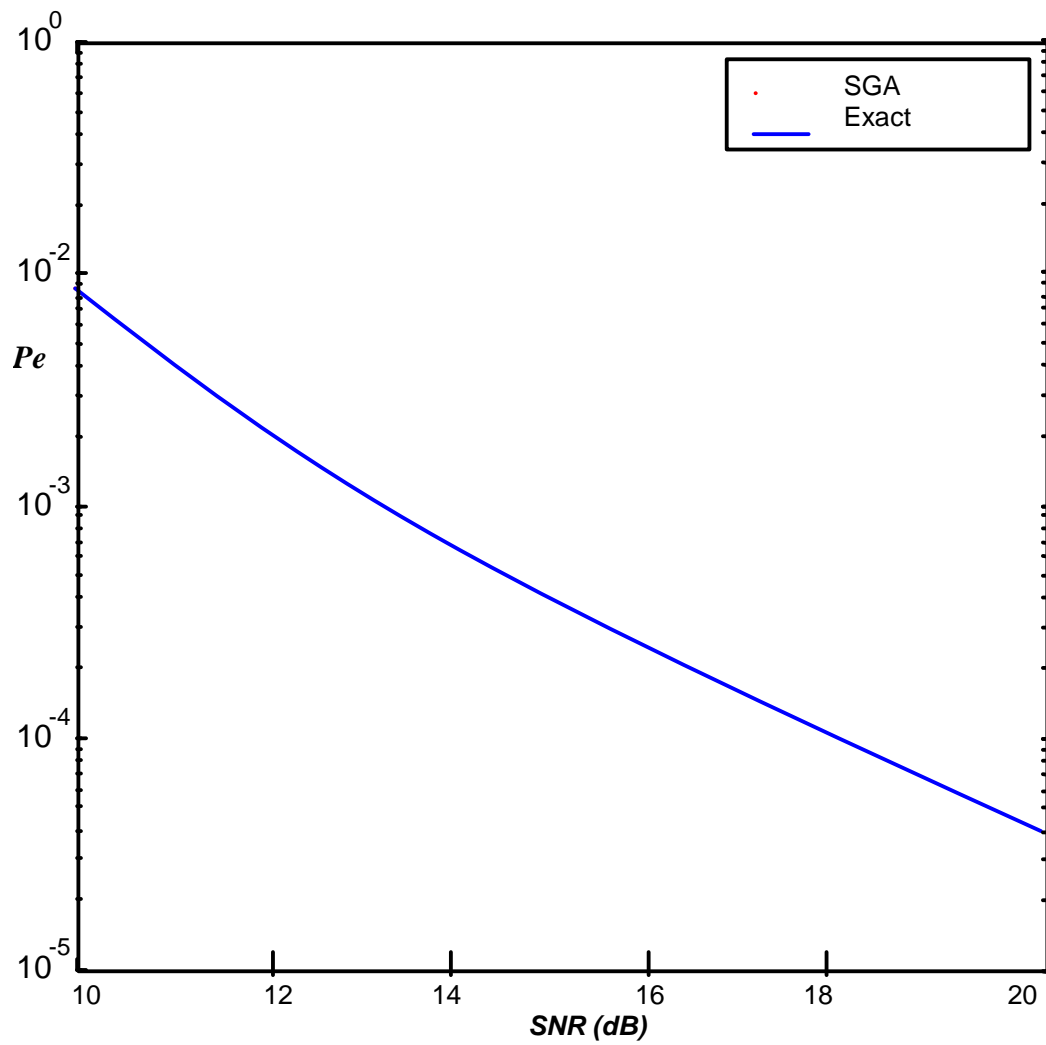


Figure 4.7. BER Performance in Multi User System, Exact and Gaussian Approximation

We notice from Figure 4.7 that at a relatively low signal to noise ratio, around 10 to 25 dB, the Standard Gaussian Approximation (SGA) of the MAI term is relatively accurate.

If the set of power levels for the $K-1$ interfering users is constant, $\mathbf{g} = \mathbf{g}$ we obtain the new approximate equivalent SNR as [66]

$$\mathbf{g}_{1eq}^- \approx \left(\frac{K-1}{N} + \frac{1}{\mathbf{g}} \right)^{-1} \quad (4-27)$$

In other words we can define a combined noise and interference term variance such that

$$\mathbf{s}_x^2 = \mathbf{s}_z^2 + \mathbf{s}^2 \mathbf{h} \quad (4-28)$$

Therefore, we can replace N_0 in (4-3, 4-6) with (4-27) where the new noise term is the combination of the thermal noise and the approximation for the MAI.

By comparing (4-24) to (4-5), we conclude that our multi-user system can be approximated relatively accurately with the SGA to a single user system where the MAI is imbedded into the total noise term for calculation of the SNR. Consequently, if we were applying our proposed adaptive power and rate control in the multi-user system, the analytical results would be very similar to the single user system. In this case, the error probability performance of our adaptive system will become (4-11) for three regions and similarly will become (4-12) for higher number of regions.

These findings can be demonstrated and validated with accurate simulations for a 2-user system where we model actual MAI in our results. We present performance

curves when the system operates in a 3-region TPC scheme and a 3-dB power adjustment policy in the next chapter.

Chapter Five:

Simulation Results

5 Simulations Results

We evaluated the performance of our proposed algorithm in the context of a W-CDMA system using a detailed block diagram simulation package called CAPSIM [67]. The CAPSIM simulation package, with its graphical interface, allows the implementers to modify simulation parameters of each block in the graphical mode. CAPSIM is a multi-rate simulation tool that is capable of modeling very complex communication systems with a large number of data points for capturing very accurate statistical results which is important for calculating the probability of error. All major components of the W-CDMA system were modeled and simulated including an accurate model for realistic flat fading mobile channels.

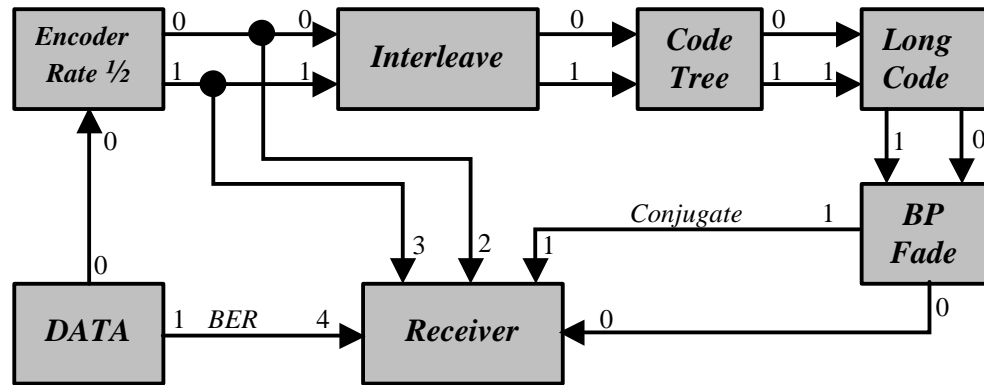


Figure 5.1. Block Diagram of Simulation Topology for W-CDMA System

In our simulation, the MS and BS transmitters randomly generate data for several seconds at 256 kbps. The output of the *DATA* block is connected to a rate $\frac{1}{2}$ convolutional

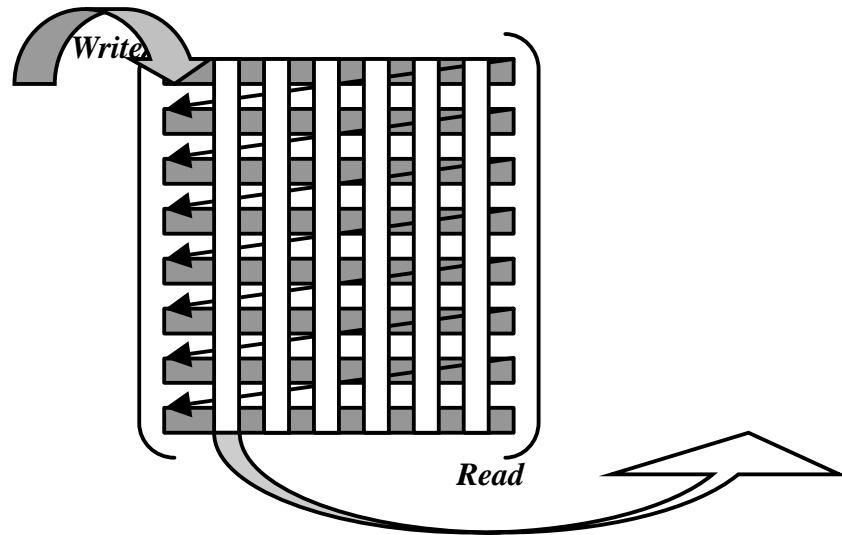


Figure 5.3. Block Interleaving

We consider that the pilot information is multiplexed with the interleaved data before appropriate orthogonal and long codes are multiplied by the signal before modulation. The data rate is assumed to be 256 Kbps with spreading factor equal to 16. That means each of the interleaved bits is over sampled with the appropriate orthogonal code of length 16. The orthogonal code that is generated by the tree structure is implemented in the *Code Tree* block where terminals 0 and 1 of the block carry the real and imaginary values of the baseband data respectively.

Our proposed SRC and TPC algorithms at the transmitter are implemented in the *Code Tree* block where the variable SF is used to create higher or lower data rates in the SRC technique or TPC values are adjusted according to the algorithm outlined previously. We assumed that the instantaneous channel power values are available at the beginning of every W-CDMA slot. Consequently, the *Code Tree* block has access to these values and makes the necessary adjustment to the rate or the power of the

transmitted slot based on rules defined by the algorithm. At the selected bit rate of 256 Kbps, the *Code Tree* block modifies the SF or the transmitted gain every 160 bits that represent one W-CDMA slot.

The next block is the *Long Code* generation where the long scrambling code is a 40960-chips segment of a Gold code of length $2^{41}-1$. The output of the spreader enters the *BP Fade* where we implemented the W. Jakes fading model. The channel is initially assumed to be flat fading with Additive White Gaussian Noise (AWGN) and later, we introduce multipath fading to the system. Figure 5.4 illustrates the *BP Fade* block diagram.

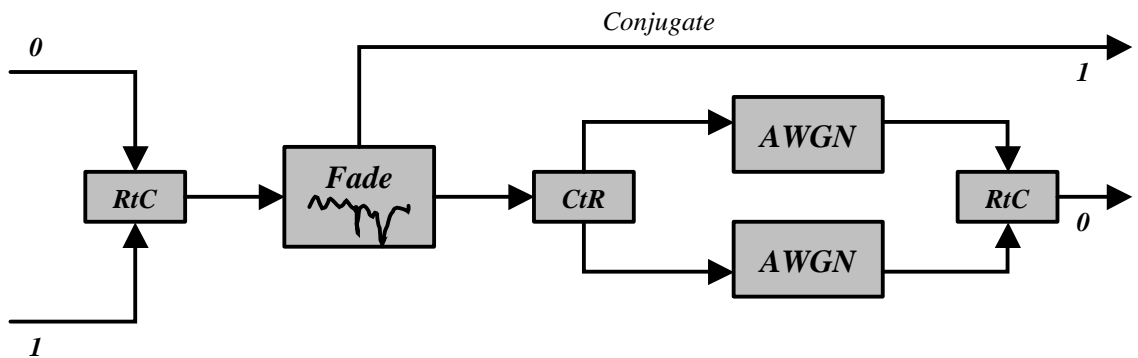


Figure 5.4. Band Pass Fading Channel Model Block Diagram

The real and the imaginary data bits from input terminals 0 and 1 undergo the *RtC* block that produces a complex value at its output terminal. The complex baseband data enters the Jakes fading channel where the channel disturbance is added to the incoming complex signal. The *Fade* block also produces the complex conjugate channel coefficients for the

RAKE receiver. The *CtR* block brings back the complex value perturbed data to Inphase and Quadrature values where the AWGN block represents the complex additive white noise at the receiver. The output terminals 0 and 1 of Figure 5.4 represent the perturbed and complex conjugate channel coefficients respectively where they enter the *Receiver* block.

The *Receiver* block uses a standard RAKE receiver with correlator banks and maximum ratio combining. For simplicity, we assume the complex conjugate channel coefficients are available to the receiver RAKE through input terminal 1 of the *Receiver* block and input terminal 0 contains the corrupted signal. Input terminals 2, 3, and 4 are used to calculate the coded and uncoded BER values.

The receiver assumes perfect knowledge of the modulation scheme. In a realistic system, some form of signaling, such as a pilot channel, must be used to convey the modulation parameters for the receiver. Figure 5.5 illustrates the block diagram of the *Receiver* block.

The complex perturbed data is initially multiplied with the complex conjugate channel coefficients provided to the *Receiver* block from the *BP Fade* Block in this simulation. The *CtR* block produces I and Q bit streams where they are multiplied by the long code that is the same as the long code applied to the transmitted data. We assumed perfect synchronization of the long spreading codes at the receiver exist. Consequently, in a multipath system where multiple instances of the perturbed data arrive at the receiver, a delayed version of the same spreading code is used to recover the data of each path.

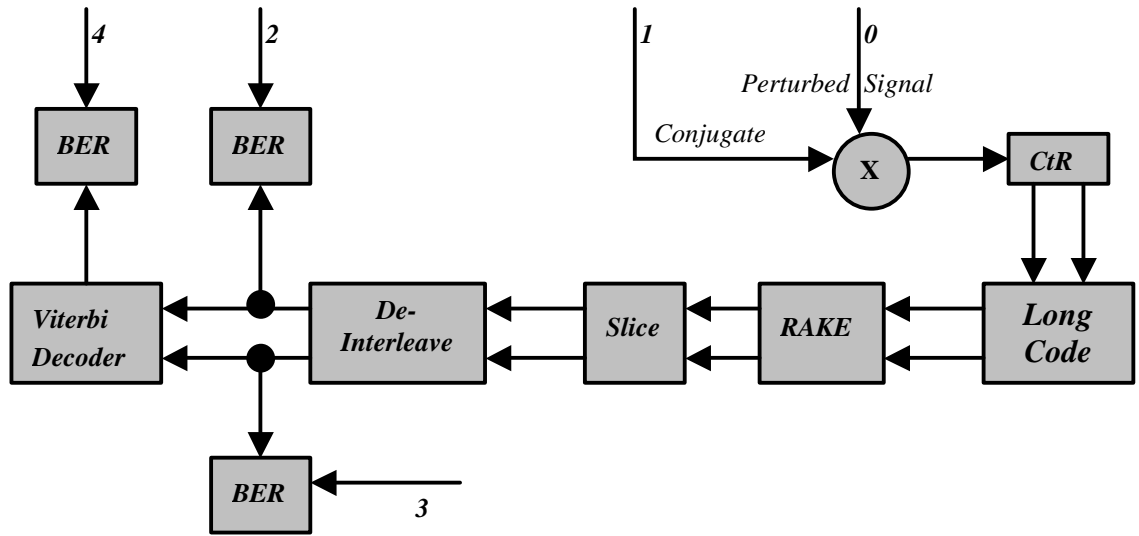


Figure 5.5. Receiver Block Diagram

The *Rake* block models the standard Maximal Ratio Combiner (MRC) RAKE receiver in the multipath Rayleigh fading operation. The output of the *Rake* block is also integrated for the length of the SF. The general block diagram of the MRC receiver is illustrated in Figure 5.6.

Figure 5.6 illustrates the operations involved in the computation of the MRC optimum receiver. The received signal $r(t)$ at each tap is correlated with the complex conjugate matched filter of $u_2^*(t)$ and $u_2^*(t)$ for the BPSK signals and convolved with the conjugate of the estimated channel coefficients $c_k^*(t)$ where $k= 1, 2, \dots, L$. In MRC, the tapped delay line receiver attempts to collect the signal energy from all the received signal paths that fall within the span of the delay line and carry the same information.

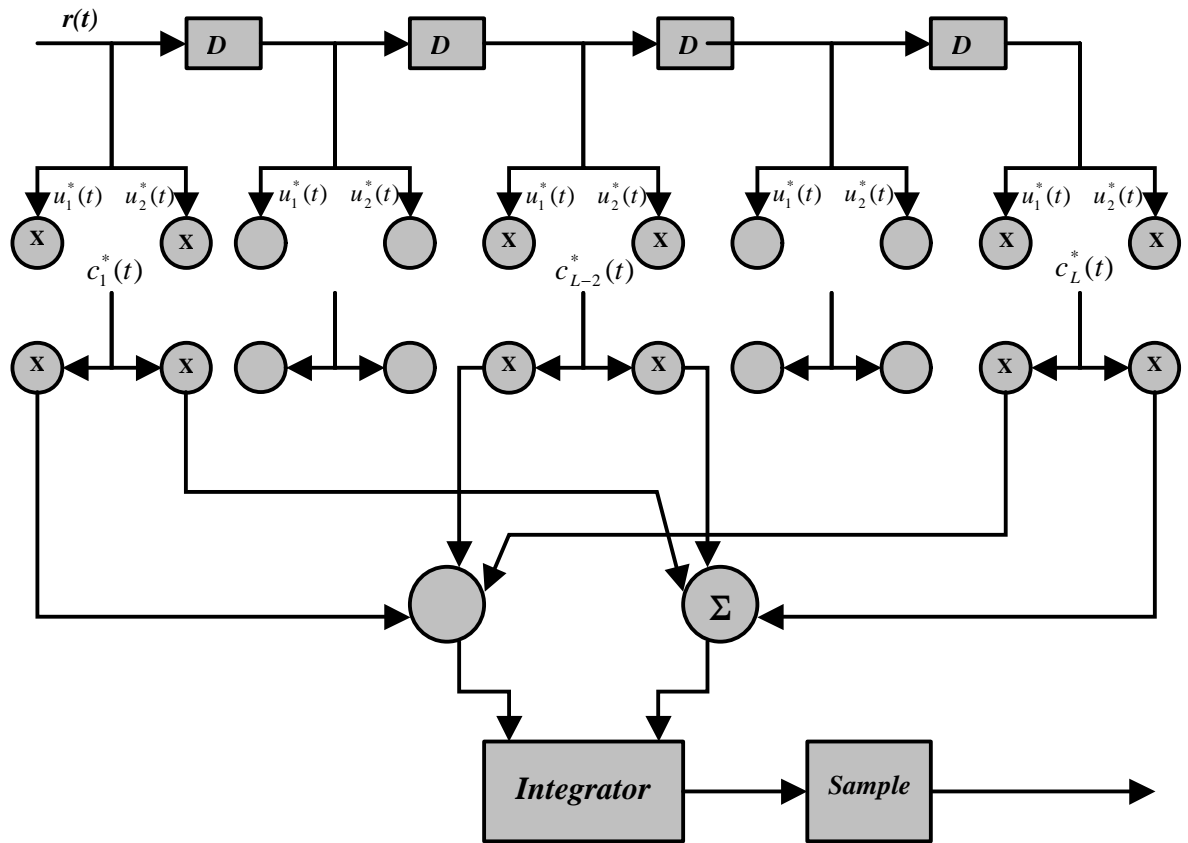


Figure 5.6. Optimum MRC for BPSK Signaling

The output of the MRC receiver is passed to the *Slice* block where the hard decisions are made based on the positive or negative values of the integrated MRC output. That is for any positive values of the MRC output, the block outputs a 1 and a 0 otherwise.

$$\begin{aligned}
 S = \sum_{j=1}^k b_k \geq 0 & \quad S_1 = 1 \\
 \text{otherwise} & \quad S_0 = 0
 \end{aligned}
 \tag{5-1}$$

In the above equation, k is the spreading factor, b is the input bit, S is the soft output and S_1 and S_0 are the hard output values.

The *De-Interleave* block performs the reverse function of the *Interleave* block. That is the data is written into columns and read in rows. The total number of bits in the *De-Interleave* and *Interleave* blocks should match. Therefore the original coded data is reconstructed at the receiver for input to the *Viterbi Decoder*.

The original data is received from input terminals 2 and 3 in Figure 5.5 and are compared with the bits received from the *De-Interleave* block in order to compute the uncoded BER at the receiver. The total uncoded BER for a BPSK is calculated by the averaging the BERs for the Inphase and Quadrature signals respectively.

The final block in Figure 5.5 is the *Viterbi Decoder*. The rate $\frac{1}{2}$ Viterbi decoder decodes the convolutionally encoded data. The output of the *Viterbi Decoder* is compared with the original data that is passed by input terminal 4.

Figure 5.7 describes the interaction between the channel prediction logic, TPC/SRC logic and the communications between the transmitter and the receiver in a practical system. This figure illustrates the block diagram of the actual receiver topology where the system operates with our proposed TPC/SRC algorithm. The *Matched filter* is matched to the shape of the transmitted symbols. The *Channel Prediction* block implements the long-range power prediction of the mobile channel. These prediction values are passed to the *TPC/SRC Logic* where the threshold values are calculated and reported to the transmitter.

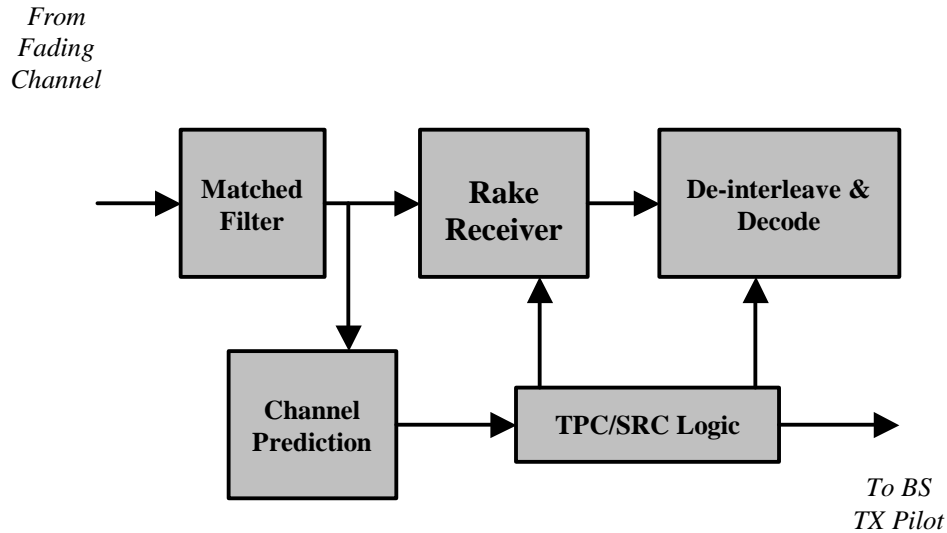


Figure 5.7. General Block Diagram of MS or BS Receiver Operating in TPC/SRC Mode

The BS Estimates the channel coefficients through the use of the transmitted pilot training symbols. The length of the pilot symbols is sufficiently adequate for estimating the complex channel coefficients and its length varies as the rate of the transmitted signal varies. Based on the linear prediction algorithm for channel power mentioned in chapter 3, the BS uses the instantaneous estimation of the complex channel coefficients to predict its long-range channel power. These predicted values are initially used to construct the channel power histogram for computing the area under the curve of the channel power pdf for 3, 5, and 7 regions for TPC or SRC. Furthermore, we computed the appropriate threshold and based on the TPC or SRC algorithm we issue a command for the remote transmitter to change its transmitter power or rate. This procedure is illustrated in Figure 5.7.

5.1 Flat Fading Performance

Figure 5.8 illustrates the error performance results of the simulation of a one-user W-CDMA system in a flat Rayleigh fading channel. In this Figure we have illustrated the error probability of the W-CDMA system with and without TPC and SRC in a three-region system.

The top curve shows the performance of the uncoded BPSK system without power or rate control. The 2nd and the 3rd curves from the top illustrate the performance of the uncoded system with TPC and SRC respectively. It is evident that the uncoded probability of error for the system operating in the TPC mode with a 3-dB adjustment policy is very similar to the system operating in the SRC mode with a doubling or halving adjustment policy. The 4th curve from the top illustrates the performance of the coded BPSK system without power or rate control. As we explained in Figure 5.2 and 5.5, the channel coding scheme is a rate $\frac{1}{2}$ convolutional encoder and rate $\frac{1}{2}$ Viterbi decoder. Similarly, the 5th and the 6th curves illustrate the performance of the coded BPSK with adaptive TPC and SRC respectively that are once again very similar. Finally the bottom curve illustrates the simulation result for the performance of the BPSK system in a AWGN channel.

Figure 5.8 also illustrates noticeable improvement in the error performance of our W-CDMA system with the TPC or the SRC schemes. We can imply from this improvement that a mobile unit with the TPC or SRC can operate at a lower transmitter power to obtain the same error probability as a system with no adaptive power or rate techniques. Lower transmitter power reflects lower MAI and consequently increases channel capacity.

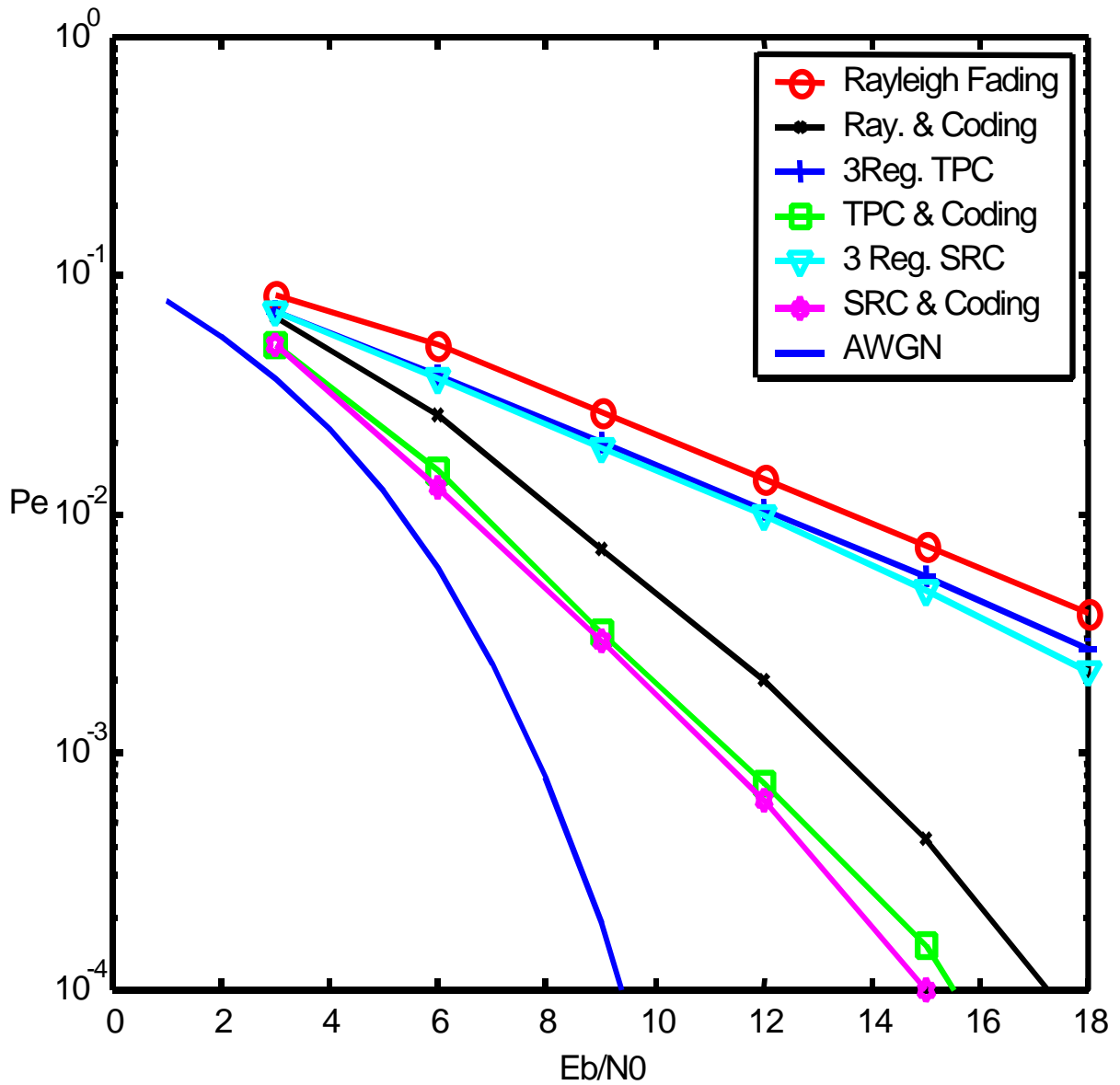


Figure 5.8. Experimental P_e vs. E_b/N_0 with/without TPC/SRC

We compared our simulation results of figure 5.8 with our analytical results that were presented in chapter 4. It is evident from these results that the simulation results of our proposed TPC and SRC technique with 3-regions of operation and a 3-dB increment

adjustment policy for the uncoded case perfectly match the theoretical results. We illustrate these results in Figure 5.9.

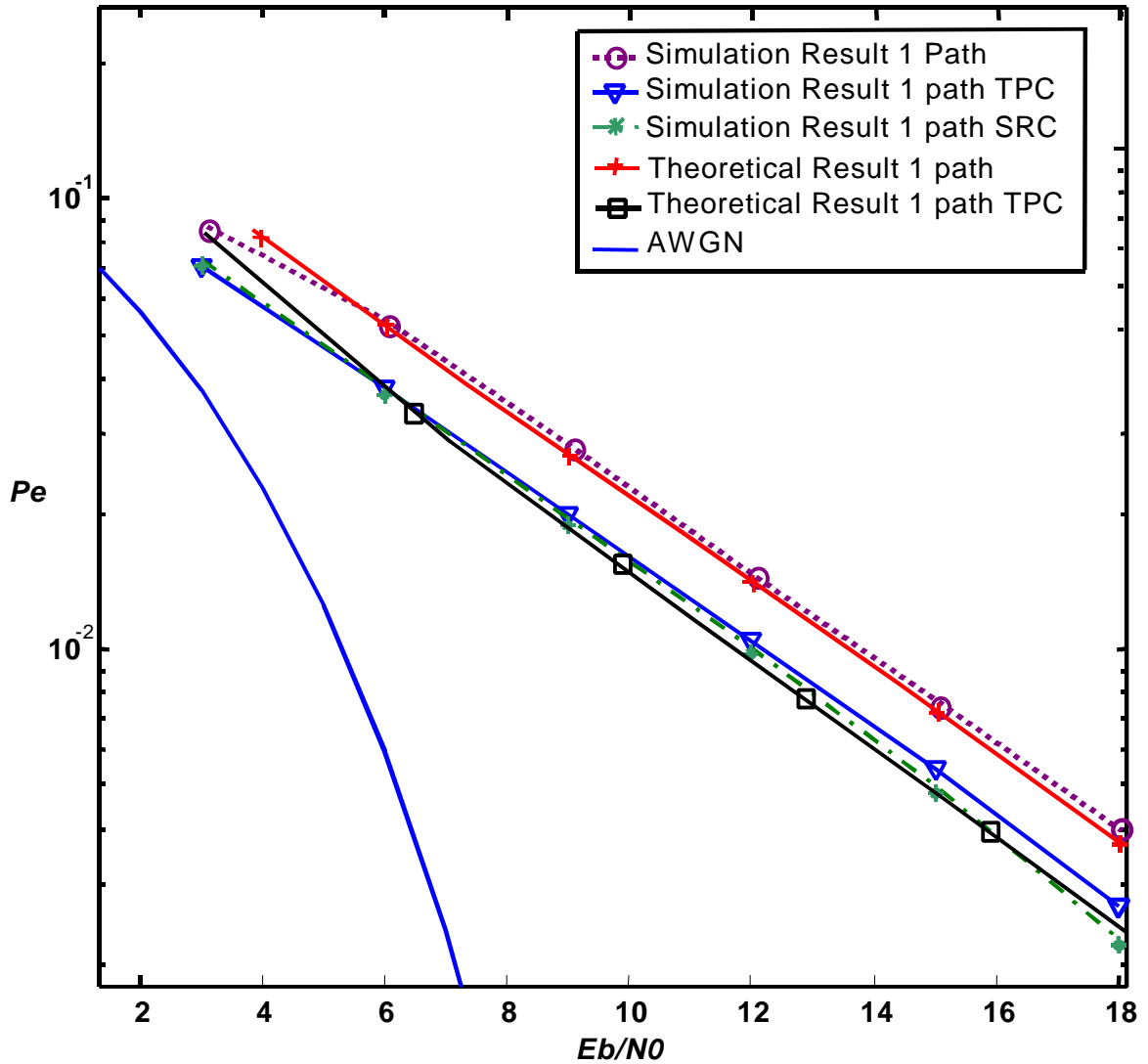


Figure 5.9. Comparison of the Simulation and the Theoretical Results for 1 Path

The top two curves in Figure 5.9 compares the theoretical error performance of our system with the simulation results. The three middle curves illustrate the performance of

the theoretical results for TPC, the simulations result for TPC and the simulation results for SRC technique. Finally the bottom curve illustrates our AWGN channel performance. Due to the limitation of our simulation environment we have not simulated beyond the 3 regions SRC and TPC. However, we conclude from the performance results shown in Figure 5.9 that in a flat fading channel environment, the 5-region and 7-region system with adaptive TPC or SRC improves the performance of the our BPSK system and reduces the error probability similar to the way it does for the 3-region policy.

5.2 Multipath Fading Performance

We simulated a one-user W-CDMA system operating in a 2-path Rayleigh fading channel model. The simulated system is very similar to the system described in Figure 5.2 with the exception of the channel model and the MRC that combines 2 fingers in the RAKE receiver. The block diagram of the multipath channel model is illustrated in Figure 5.10.

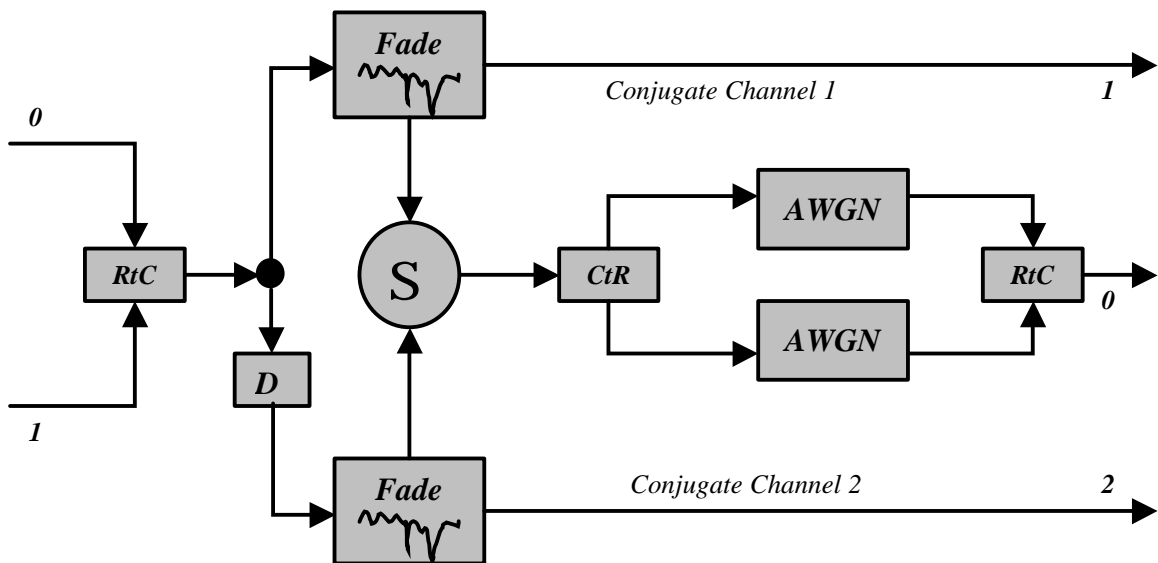


Figure 5.10. Band Pass Fading Channel Model Block Diagram

The transmitted signal that is received from input terminals 0 and 1 are convolved with the two independent complex fading channels signals that arrive at the receiver at instances delayed by 1 chip. For the two path channel model simulations, we normalized the total average channel power to 1 similarly to our one path channel model simulation where $E(\mathbf{a}^2) = 1$. We assume that both the perturbed original and the delayed version of the same transmitted signal propagated through two independent paths. A complex AWGN is applied to the combined channel coefficients to model the thermal noise at the receiver

We illustrate the error performance of our proposed technique by fixing the AWGN variance and adjusting the transmit power level to generate a range of E_b/N_0 for the BER curves. The simulated results for our TPC and SRC system are plotted in Figure 5.11. In this Figure, we illustrated the error probability of the W-CDMA system with and without TPC and SRC in a three-region system with a 3-dB step adjustment policy. The top two curves in Figure 5.11 show that when the system operates with a 2-path Rayleigh fading channel and a 2-finger MRC receiver, it performs significantly better than the system operating in a flat fading channel. Furthermore, the error performance of our system improves with a 3-region adaptive TPC or SRC and a 3-dB adjustment policy. The two bottom curves in Figure 5.11 illustrate the improved error performance of the system in conjunction with channel coding where the inherent redundancies introduced in the convolutional encoder are used to correct the random errors introduced by the channel at the decoder.

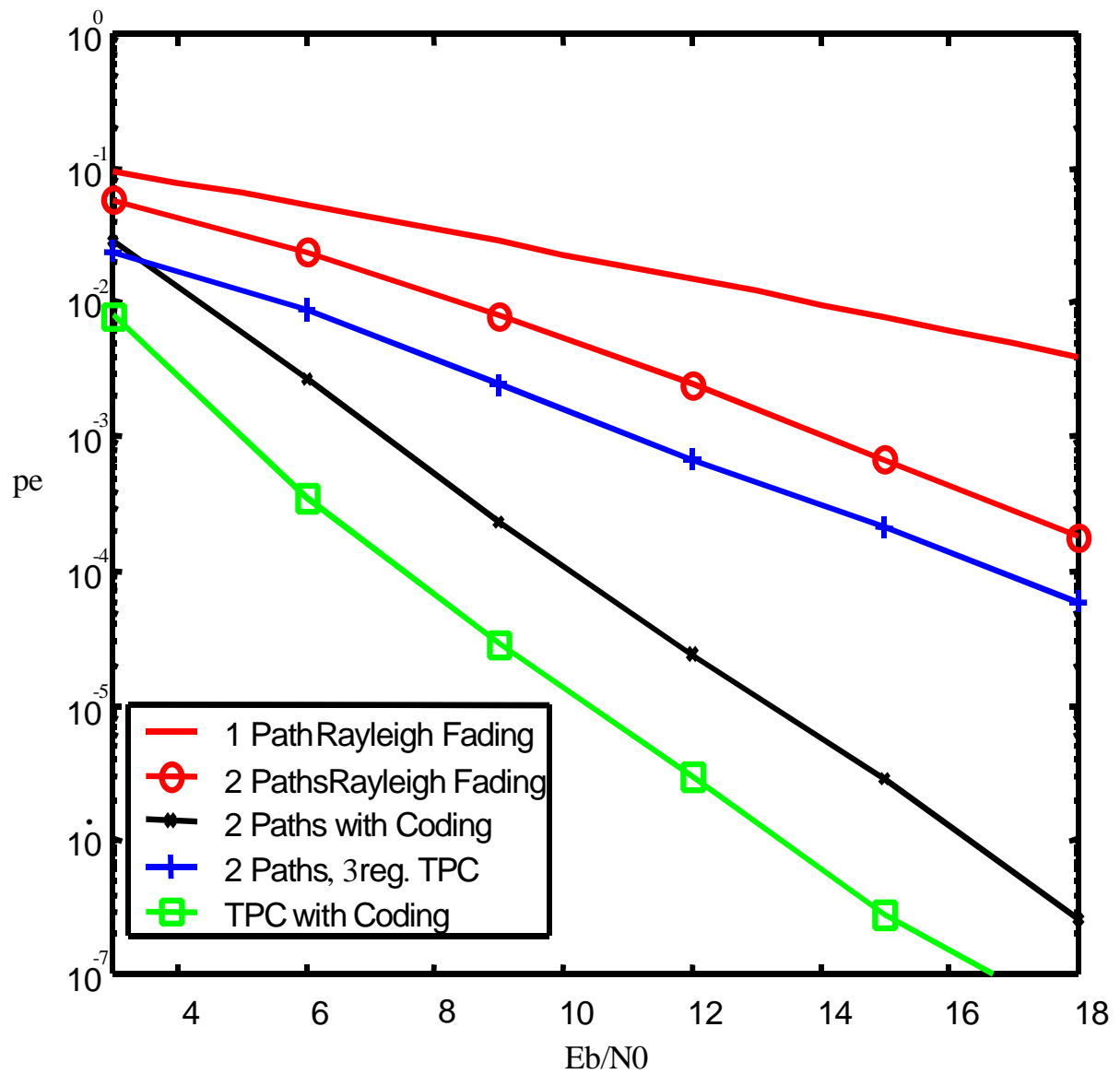


Figure 5.11. Simulation Results for P_e vs. E_b/N_0 with/without TPC/SRC, 2-Paths

Similarly to the flat fading performance comparison, the results presented in Figure 5.11 perfectly match the analytical results presented in Figure 4.6. Figure 5.12 illustrates the theoretical and the simulation results for the error performance of our W-CDMA system.

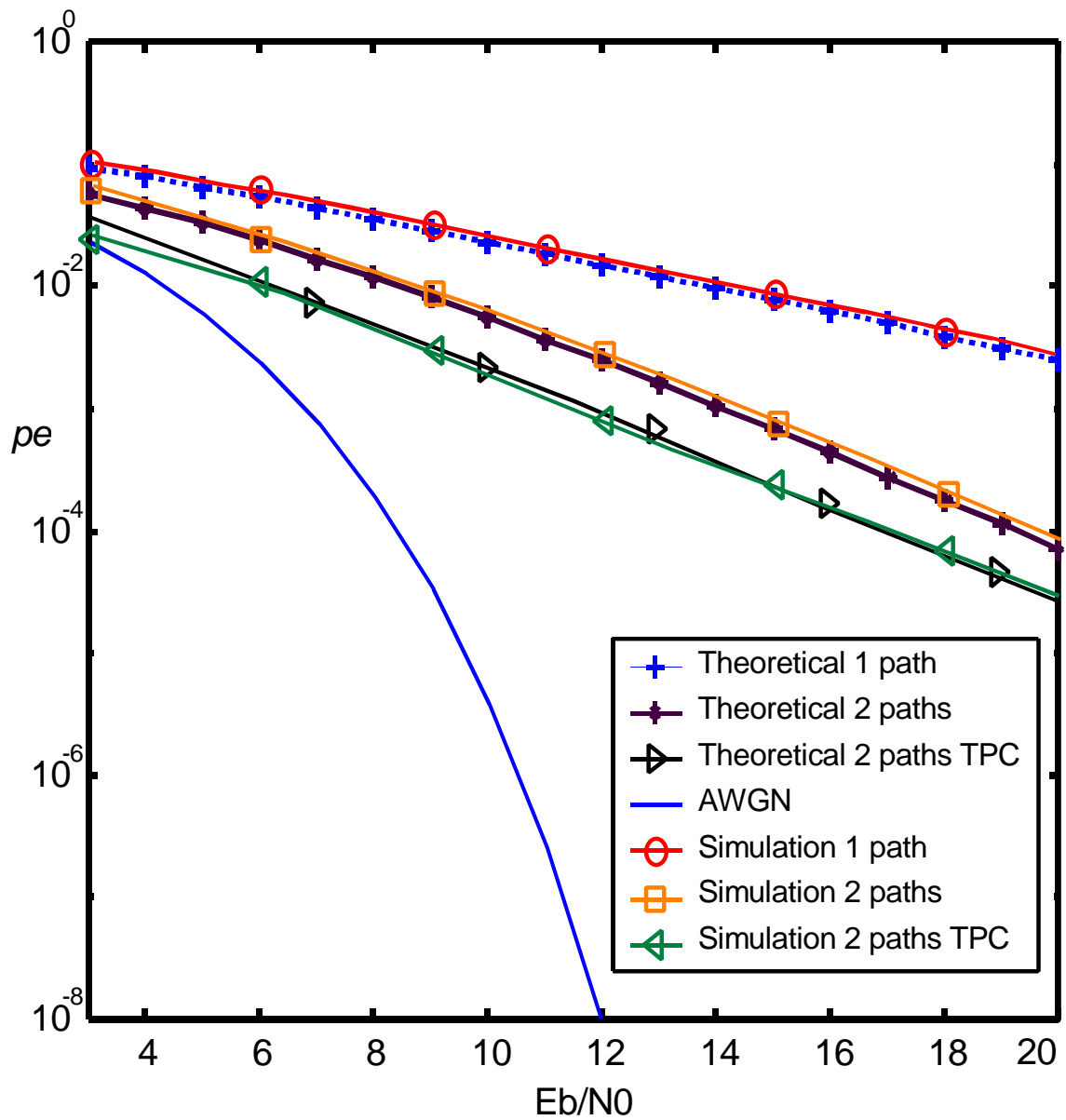


Figure 5.12. Comparison of the Simulation and the Theoretical Results for 2 Paths

The top two curves in Figure 5.12 compare the theoretical error performance of our system with the simulation results when operates in a 1-path Rayleigh fading channel. The middle two curves illustrate the error performance of the theoretical and the simulations result for our system with no power control in a 2-path fading model and the

next coupled curves are with 3-region TPC adaptive power control and 3-dB power adjustment policy. Finally the bottom curve illustrates the AWGN channel performance. Due to the limitation of our simulation environment we have not simulated beyond the 3 regions SRC and TPC. Furthermore, we conclude from the performance results shown in Figure 5.12 and Figure 4.6 that the error performance of our proposed TPC and SRC techniques improves when the number of regions increases to 5-region and 7-region in the multipath fading channel environment and MRC receiver.

5.3 Multi-user Performance

We applied the TPC technique in our simulation of a 2-user system where user 2 introduces interference to user 1. However, user 1 does not introduce interference to user 2. In this case we can monitor the effect of the MAI on user one while user 2 adjusts its transmitter power based on our adaptive TPC technique. Due to the fact that the performance of the TPC technique with 3-dB adjustment policy is similar to the SRC technique, we have not performed simulations for our proposed SRC technique. However, it is clear from the derivations and the illustrations in this chapter that their performance is very similar. Figure 5.13 illustrates the block diagram of a 2-user system.

In this block diagram, user 1 and user 2 identically perform the transmitter and receiver function of 2 mobile units. In this configuration we assume that user 2 introduces MAI to user 1. Both users operate at the same transmission rate with two distinct orthogonal codes. The transmitted data is spread using 2 unique long codes initialized with different seeds for the uplink transmission to the base station. Each user propagates data through independent flat fading channels in this simulation.

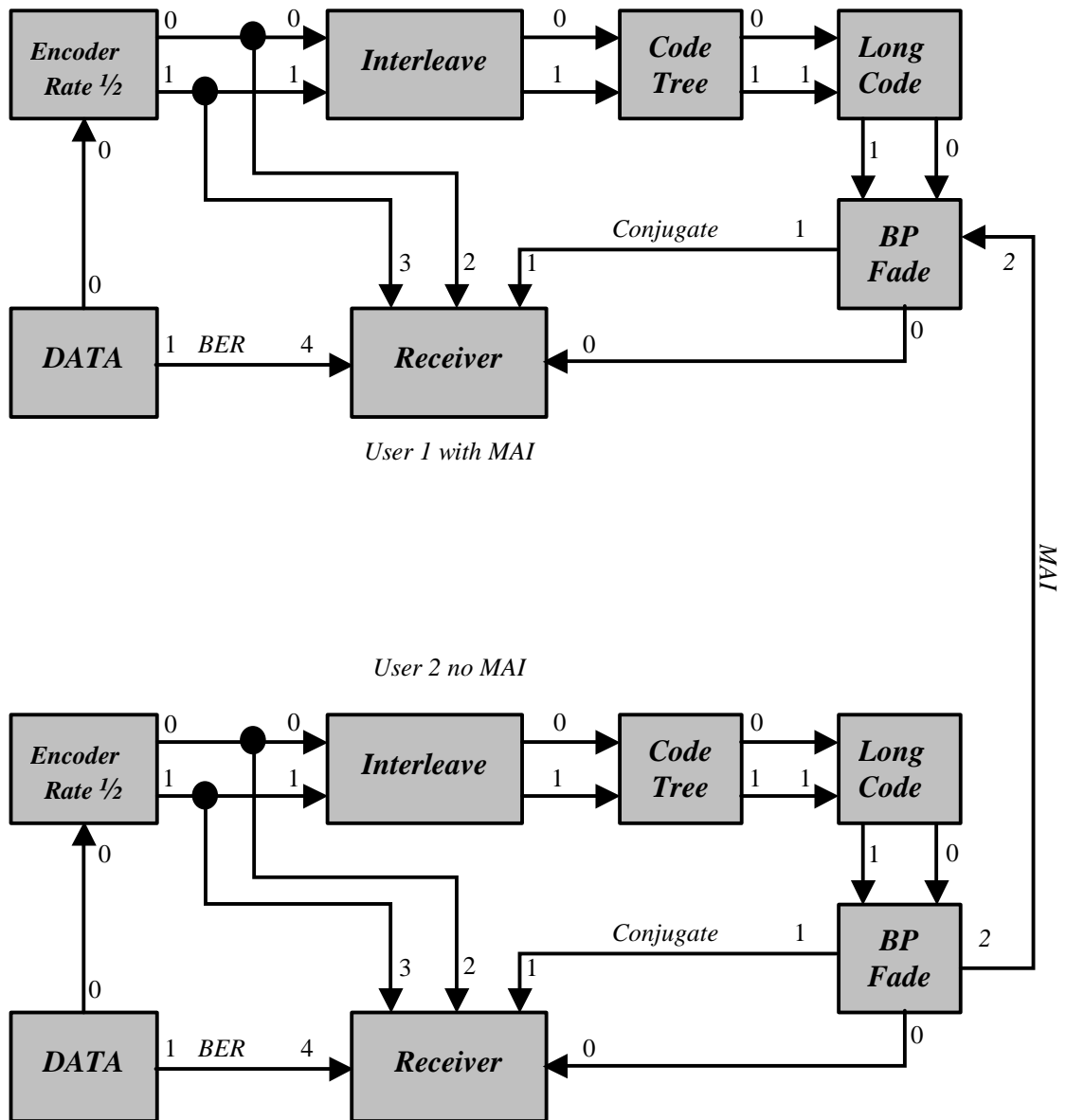


Figure 5.13. Top Level Block Diagram of a 2-User W-CDMA system

The *BP Fade* block for user 2 is similar to Figure 5.4 with the exception of a second output that contains the MAI. However, topology of the *BP Fade* block for user 1 is

different from the topology of the *BP Fade* block of user 2 in the sense that it receives MAI from the output terminal 2 for *BP Fade* block for user 2. The diagram of *BP Fade* block for user 1 is illustrated in Figure 5.14.

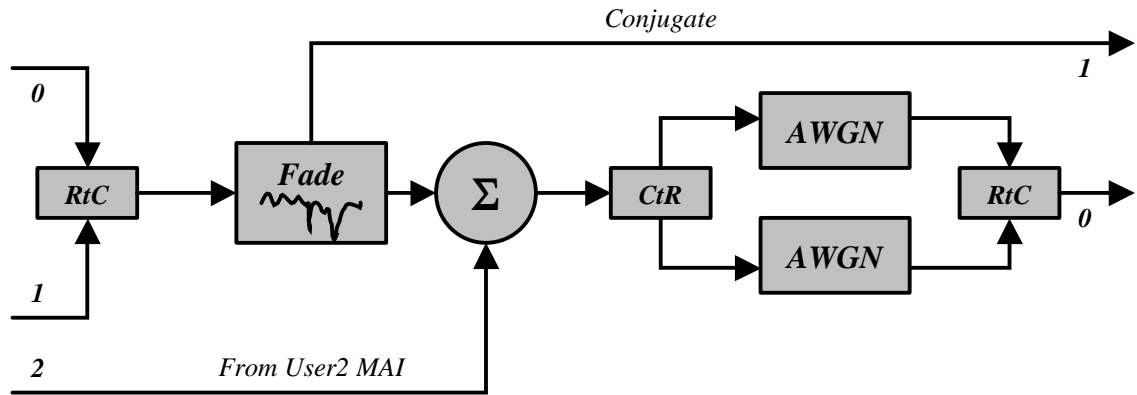


Figure 5.14. Band Pass Fading Channel Model with MAI

In the traditional single user detector for multi-user systems, the closed-loop power control tries to compensate the deep fades in the channel by increasing the transmit power to the point that the SNR at the receiver becomes acceptable. Due to the time variant nature of the mobile radio channel, if the power control is not performed effectively, it increases the near far effect.

However, in our proposed power and rate control schemes, the total average interference power remains constant, due to the selected regions of operation that is based on the channel power pdf. Consequently, the effect of the near-far problem is practically reduced or eliminated. Figure 5.15 illustrates the error performance of our two-user system in conjunction with our proposed three-region TPC and 3-dB adjustment policy.

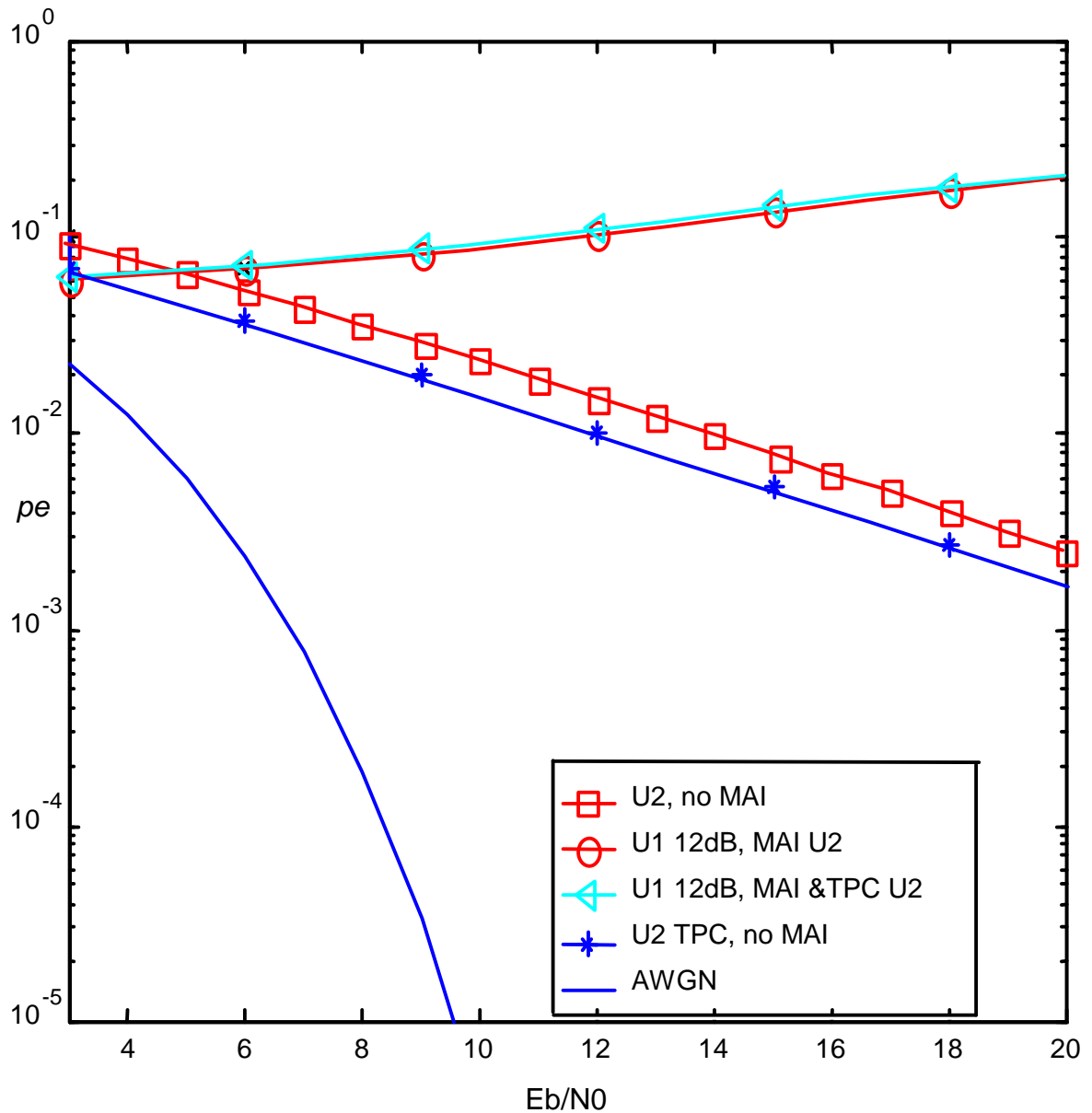


Figure 5.15. Simulation Results for P_e vs. E_b/N_0 , 2-User Performance, Constant Power User 1

The top two curves in Figure 5.15 illustrate the error performance of the user 1 with MAI from user 2. In this simulation, user 1 is operating at a constant 12 dB transmit SNR where user 2 increases its transmitter power from 3 dB to 20 dB. The bottom two curves show the performance of user 2 without MAI from user 1 and finally, the last curve is the

performance of user 2 in the AWGN channel. We notice from these curves that the error performance of user 1 remains constant while user 2 applies TPC at the transmitter.

We also conducted another simulation where user 1 operates at the same transmit SNR level as user 2. In this simulation both users increase their transmitter power from 3 dB to 20 dB. Figure 5.16 illustrates the error performance of this system.

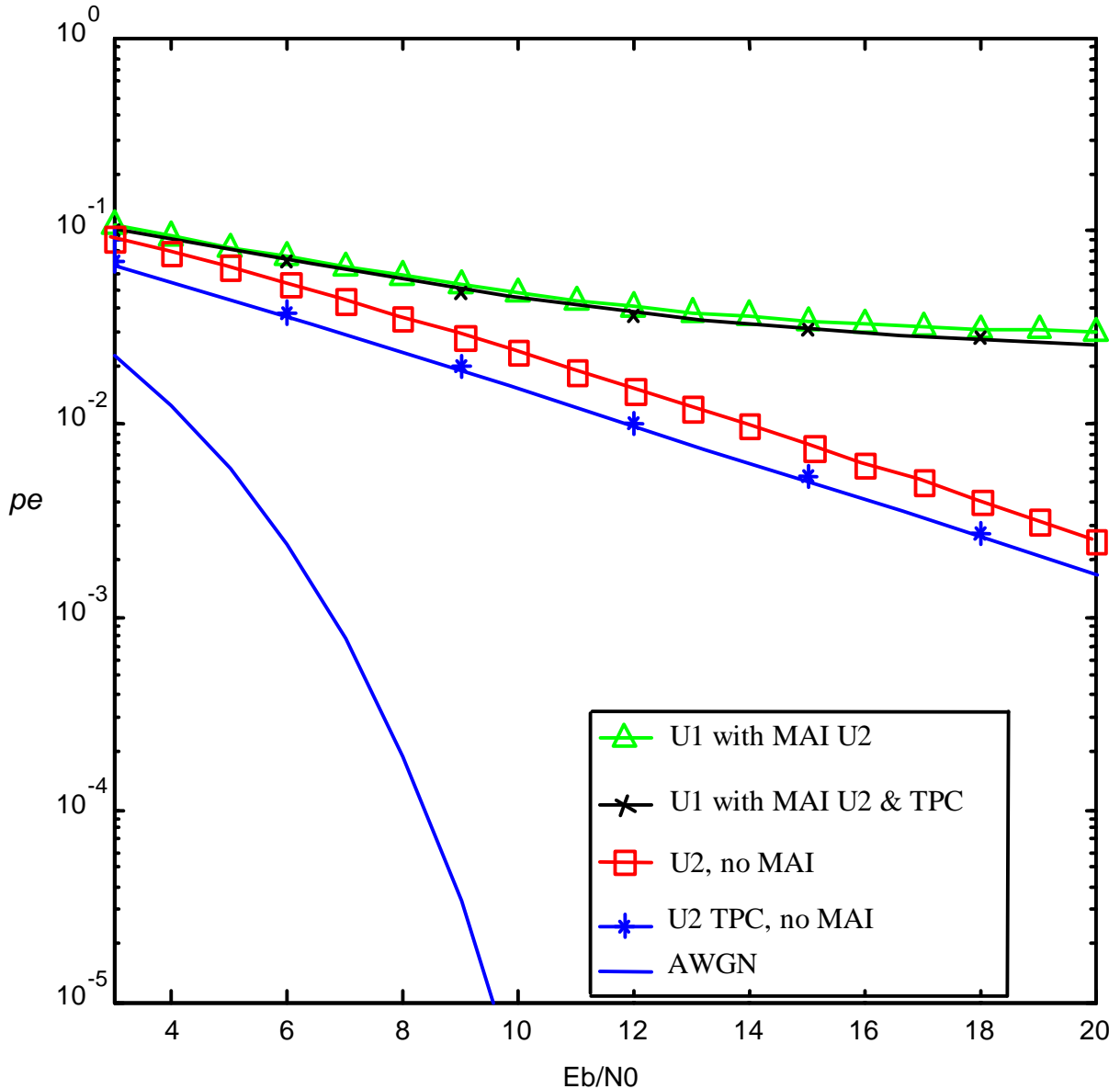


Figure 5.16. Simulation Results for P_e vs. E_b/N_0 , 2-User Performance, Equal Power

The top two curves in Figure 5.16 are similar to the top two curves in Figure 5.15, where they illustrate the error performance of user 1 with the MAI from user 2. The middle two curves illustrate the error performance of user 2 without MAI from user 1 and finally, the last curve shows the error performance of user 2 in the AWGN channel.

Consequently, by comparing and analyzing Figure 5.15 and Figure 5.16, it is apparent that the error performance of our 2-user system improves when the TPC technique is applied to every user. We also notice from these curves that the error performance for user 1 remains constant while user 2 applies TPC at the transmitter.

One can generalize from these error performance results that as the number of users increases, the amount of MAI power also increases. Therefore, since the capacity of CDMA systems are interference limited, as we showed in our 2-user system, the TPC or SRC technique reduces the MAI. Therefore, we conclude that in a W-CDMA system when all users adopt our adaptive TPC or SRC schemes, we obtain the same SNR value at the receiver with a smaller transmitter power. Consequently, the total channel capacity increases and the error performance of each user in the system improves noticeably.

Chapter Six:
Conclusions and Future
Work

6 Conclusion and Future Work

We have proposed novel adaptive power and rate control techniques for W-CDMA systems according to an algorithm for long-range prediction of the mobile channels. We simulated all major components of the system including the channel coding, interleaving, spreading and accurate model of flat and multipath Rayleigh fading channels.

We performed extensive background literature and patent search regarding the past and present state of the adaptive power and rate control in the CDMA and W-CDMA systems. Based upon our literature review, we defined an enhancement to the existing power and rate control technique for W-CDMA systems. Our analytical and simulation results show that our proposed techniques would reduce the system's probability of error, reduce the MAI and consequently increase the channel capacity.

We defined a mobile system with three regions of operations (0-A, A-B, B- ∞). These regions are defined based upon the mobile channel power pdf. The operation of the system is such that the mobile station transmitter modifies its transmitter power by multiplying its transmitted symbols by a set gain factor during its operation in each region. Furthermore, it can modify its transmitter rate by doubling or halving its spreading factor. The thresholds in our simulated system were set such that the system operates 33% of time in the low-power region [0, A), 33% in the mid-power region [A, B) and 33% in the high-power region [B, ∞).

We were able to formulate the problem in a mathematical model and we presented comprehensive analytical results to support our findings. Furthermore, we demonstrated that the simulation results accurately match the analytical results. We show

that the use of our techniques in conjunction with channel coding can further improve the system performance and reduce the probability of error. We also described a method to improve the channel capacity by dynamically reducing the transmit rate to allow temporary admission of new users to the system.

We extended the proposal to a multipath environment where power and rate control thresholds are set according to the pdf of the multipath channel power. We approximated the MAI in a multi-user environment as a standard Gaussian approximation and demonstrated that the proposed technique reduces the multi-access interference while keeping the average BER constant.

The practical applications of our techniques are in W-CDMA systems where higher bandwidth, better throughput and increase in the channel capacity are the goals of the promoters of the third generation mobile system. We rely vastly on the accurate long-range power prediction of the mobile channel to perceive the maximum performance of our proposed techniques. However, we did not address the long-range power prediction problem in this dissertation.

Due to the fact that we have assumed a perfect channel power prediction in our simulations of our power and rate control algorithm, a possible future research contribution could be to extend the long-range channel power prediction scheme by solving a nonlinear model that may forecast more accurate prediction coefficients. A more accurate long-range channel power prediction would lead to a more accurate channel power pdf, which could be more beneficial in our proposed technique.

Another possible enhancement to the W-CDMA system is the use of an adaptive coding technique in conjunction with our proposed power and rate control schemes where

the combination can provide a basis for a communication system that may fully exploit the potential capacity of the mobile radio channel. A different number of regions can also be explored where the system can adjust its configuration based on the new set of defined regions. Generally speaking, any increase in spectral efficiency in mobile telephony would allow more mobile units to access the same base station. Consequently, a lower transmit power requirement would be associated with longer talk times and would reduce MAI.

References

7 References

- 1 B. Lindof, C. Ostberg, and H. Eriksson, "Channel Estimation for the W-CDMA System, Performance and Robustness Analyses from a Terminal Perspective," *IEEE Vehicular Technology Conference. Document 90. May 1999.*
- 2 B. Jabbari, "Wideband CDMA," *IEEE Communications Magazine*, pp. 46-68, September 1998.
- 3 E. Dahlman, P. Beming, J. Knutsson, F. Ovesjo, M. Persson, and C. Roobol, "WCDMA- The Radio Interface for Future Mobile Multimedia Communications," *IEEE Transaction on Vehicular Technology, Vol. 47. No. 4, Pp. 1105-1117, November 1998*
- 4 M. Zeng, A. Annamalai, and V. K. Bhargava, "Recent Advances in Cellular Wireless Communications," *IEEE Communications Magazine, Vol. 37, No. 9, September 1999, pp. 128-138.*
- 5 J. F. Hayes, "Adaptive Feedback Communications," *IEEE Transaction on Communications Technology, Vol. COM-16, pp 29-34, February 1968.*
- 6 M. Alouini, and A. Goldsmith, "Capacity of Rayleigh Fading Channels Under Different Adaptive Transmission and Diversity-Combining Techniques," *IEEE Transaction on Vehicular Technology, Vol. 48. No. 4, Pp. 1165-1181, July 1999.*
- 7 M. Alouini, X. Tang and A. Goldsmith, "An Adaptive Modulation Scheme for Simultaneous Voice and Data Transmission over Fading Channels," *IEEE Vehicular Technology Conference, pp. 939-943 November 1998.*
- 8 C. C. Lee, R. Steele, "Closed-loop Power Control in CDMA Systems," *IEE Proc. Communications, Vol. 143, No. 4, August 1996.*
- 9 M. Sim, Ee. Gunawan, B. Soong, and CCh. Soh, " Performance Study of Closed-Loop Power Control Algorithms for a Cellular CDMA System," *IEEE Transaction on Vehicular Technology, Vol. 48. No. 3, Pp. 911-921, May 1999.*
- 10 J. M. A. Tanskanen, A. Huang, and I.O. Hartimo, "Predictive Power Estimators in CDMA Closed Loop Power Control," *IEEE Vehicular Technology Conference, pp. 1091-1095, April 1998.*

-
- 11 P. Agrawal, B. Narendran, J. Sienicki and S. Yajnik, "An Adaptive Power Control and Coding Scheme for Mobile Radio Systems," *IEEE ICPWC*, pp. 283-288, 1996.
 - 12 A. Sampei, N. Morinaga, and Y. Kamio, "Adaptive Modulation/TDMA with BDDFE for 2 Mbit/s Multi-Media wireless communication systems, *IEEE Vehicular Technology Conference*, pp. 311-315/1091-1095, July 1995.
 - 13 T. Ue, S. Sampei, N. Morinaga, and K. Hamaguchi, "Symbol Rate and Modulation Level-Controlled Adaptive Modulation / TDMA / TDD System for High-Bit-Rate Wireless Data Transmission," *IEEE Transaction on Vehicular Technology*, Vol. 47, No. 4, Pp. 1134-1147, November 1998.
 - 14 S. Abeta, S. Sampei, and N. Morinaga, "Adaptive Coding and Processing Gain Control with Channel Activation for Multimedia DS/CDMA System," *IEICE Transaction on Communication*, Vol. E80-B, No. 4, April 1997.
 - 15 T. ITO, S. Sampei, and N. Morinaga, "A Wireless Packet Transmission with Adaptive Processing Gain and Transmitter Power Control Scheme for Circuit-Switched and Packet-Switched Modes Integrated DSS/CDMA Systems," *IEEE Vehicular Technology Conference*, pp. 2038-2043, July 1999
 - 16 C.H. Wong, and L. Hanzo, "Upper-bound Performance of a Wideband Burst-by-Burst Adaptive Modem," *IEEE Vehicular Technology Conference. Document 483, CD-ROM*, July 1999.
 - 17 E. Tiedemann, Jr. et al, "U.S.P. 5,822,381" issued October 13, 1998.
 - 18 L. A. Weaver, Jr., et al, "U.S.P. 5,715,526" issued February 3, 1998
 - 19 C. E. Wheatley, III, et al, "U S.P. 5,383,219" issued January 17, 1995.
 - 20 S.H. Gardner, et al, "U.S.P. 5,729,557" issued March 17, 1998.
 - 21 Tetsuyoshi et al, "JP6-276176" published September 30, 1994.
 - 22 A. Goldsmith and S. Chua, "Variable-Rate Variable-Power MQAM for Fading Channels," *IEEE Transaction on Communications*, VOL. 45, No. October 1997.
 - 23 T. Eyceoz, A. Duel-Hallen, and H. Hallen, "Deterministic Channel Modeling and Long Range Prediction of Fast Mobile Radio Channels," *IEEE Communication Letters*, Vol. 2, No. 9, September 1998.
 - 24 J. K. Cavers, "An Analysis of Pilot Symbol assisted Modulation for Rayleigh Fading Channels," *IEEE Transaction on Vehicular Technology*, Pp. 686-693, Nov. 1991.

-
- 25 P. A. Bello, "Time-Frequency Duality," *IEEE Transactions on Information Theory*, vol. IT-10, pp. 18-33, January 1964.
 - 26 P. A. Bello, "Characterization of Randomly Time-Variant Linear Channels," *IEEE Transactions on Communications Systems*, Vol. CS-11, pp. 360-393, December 1963.
 - 27 A. Papoulis, *Probability, Random Variables, and Stochastic Processes*, 3rd edition, McGraw-Hill, New York, 1991.
 - 28 W. C. Lee, *Mobile Communications Engineering*, McGraw-Hill, New York, 1998.
 - 29 A. Sathyendran, K. W. Sowerby, and M. Shafi, "Capacity Estimation for 3rd Generation CDMA Cellular Systems," *IEEE Vehicular Technology Conference. Document 74, CD-ROM*, July 1999.
 - 30 W. C. Jakes, *Microwave Mobile Communications*. Piscataway, NJ: IEEE Press, 1993.
 - 31 P. Den, G. E. Bottomley, and T. Croft. "Jakes Fading Model Revised," *Electronics Letters*, 29(13), pp. 1162-1163, June 1993.
 - 32 T. S. Rappaport, *Wireless Communications*. Upper Saddle River, NJ. Prentice Hall, 1999.
 - 33 T. Eyceoz, Sh. Hu, A. Duel-Hallen, and H. Hallen, "Adaptive Prediction, Tracking and power adjustment for frequency Non-Selective Fast Fading Channels," *Eight Communication Theory Mini-Conference CTMC*, 1999.
 - 34 Q. Shen, B. Wu, A. Elhakeem, *Wireless Personal Communications*, The Netherlands: Kluwer Academic Publishers, 1998.
 - 35 G. R. Cooper, and C. D. McGillem, *Modern Communications and Spread Spectrum*, New York, McGraw-Hill Book Company, 1986.
 - 36 V. K. Garg, K. Smolik, and J. E. Wilkers, *Applications of CDMA in Wireless/Personal Communications*, Upper Saddle River, NJ. Prentice Hall, 1997
 - 37 A. Sadri, A. Dholakia, "Equalization, Coding and Diversity Combining for TDMA Digital Cellular System," *IEEE Vehicular Technology Conference 45th*, Vol. 1, P. 404-408, 1995.
 - 38 EIA.TIA Interim Standards, "Cellular System Dual Mode Mobile Station – Land Station Compatibility Specifications," *IS-54*, *Electronic Industries Association*, May 1990.

-
- 39 A. Sadri, P. Yegani, "Comparison of Adaptive Diversity Receivers for TDMA Digital Mobile Radio," *Vehicular Technology Conference, Vol. 2, pp.1276 –1280, 1994.*
- 40 M. K. Simon, J. K. Omura, R. A. Scholtz and B. K. Levitt, "*Spread Spectrum Communications Handbook,*" New York: McGraw Hill, 1994.
- 41 EIA TIA Standards, "Mobile Station-Base Station Compatibility Standard for Dual Mode Spread Spectrum Cellular System," *IS-95-A, Electronic Industries Association.*
- 42 E. Nikula, A. Toskala, E. Dahlman, L. Girard, and A. Klein, "Frame Multiple Access for UMTS and IMT2000," *IEEE Pers. Commun. , Vol. 5, April 1998.*
- 43 "UMTS 30.01 Baseline Document," *ETSI SMG#23, Budapest, Hungary, October 13, 1997.*
- 44 E. Dahlman, P. Beming, J. Knutsson, F. Ovesjo, M. Persson, C. Roobol, "WCDMA-The Radio Interface for Future Mobile Multimedia Communications," *IEEE Transaction on Vehicular Technology, Vol. 46, No. 4, Nov. 1998.*
- 45 F. Adachi, M. Sawahashi and K. Okawa, "Tree-Structured Generation of Orthogonal Spreading Codes with Different Length for Forward Link of DS-CDMA Mobile Radio," *Elec. Lett. Vol.33, no. 1, pp. 27-28, Jan. 1997.*
- 46 E. Dinan and B. Jabbari, "Spreading Codes for Direct Sequence CDMA and Wideband CDMA Cellular Networks," *IEEE Communications Magazine, pp48-54, September 1998.*
- 47 3rd Generation Partnership Project., "Spreading and Modulation (TDD)," *Technical Specification Group Radio Access Network, 3G TS 25.223, V3.1.0, December 1999.*
- 48 T. Kasami, "Weight Distribution Formula for Some Class of Cyclic Codes," *Coordinated Science Lab. Univ. IL. Urbana. Tech. Rep., R-285, April 1966.*
- 49 R. Gold, "Optimal Binary Sequences for Spread Spectrum Multiplexing," *IEEE Transaction on Information Theory, Vol. IT-B, pp. 619-621, Oct. 1967.*
- 50 D. H. Won, W. W. Kim, and I. M. Jeong, "Performance Improvement of CDMA Power Control in Variable Fading Environment," *IEEE Southeast Conference, pp. 241-243, 1997.*
- 51 A. Sadri, T. Eyceoz and W. Alexander, "Adaptive Transmitter Power Control (TPC) and Seamless Rate Change (SRC) in Wideband Direct Sequence Multiple Access Systems," *AP2000 Millennium Conference on Antennas & Propagation, April 2000.*

-
- 52 A. Sadri, T. Eyceoz and W. Alexander, "Novel Adaptive Transmitter and Power Control in 3rd Generation W-CDMA Systems," *To appear in the Vehicular Technology Conference, May 2000.*
- 53 J. K. Cavers, "Variable-Rate Transmission for Rayleigh Fading Channels," *IEEE Transaction on Communications,* Vol. COM-20, pp 15-22, February 1972.
- 54 W. T. Webb, and R. Steele, "Variable Rate QAM for mobile Radio," *IEEE Transaction on Communications,* Vol. 43, pp 2223-2230, July 1995.
- 55 B. Vucetic, "An Adaptive Coding Scheme for Time-Varying Channels," *IEEE Transaction on Communications,* Vol. 39, pp 653-663, May 1991.
- 56 L. C. Yun and D. G. Messerschmitt, "Variable Quality of Service in CDMA System by Statistical Power Control," *IEEE international communications Conference,* pp. 713-719, June 1995.
- 57 Y. Okumura and F. Adachi, "Variable Rate Transmission and Blind Rate Detection for Coherent DS-CDMA Mobile Radio," *Electronics Letter,* Vol. 33 pp. 2026-2027, November 1997.
- 58 John Proakis, *Digital Communications,* New York: McGraw Hill, 1995.
- 59 Mathematica, "Wolfram Research, Inc." Champaign, Illinois, 1998.
- 60 Alberto Leon-Garcia, *Probability and Random Processes for Electrical Engineering,* New York: Addison Wesley, 1994.
- 61 Sergio Verdu, *Multiuser Detection,* Cambridge. Cambridge University Press 1998.
- 62 H. Vincent Poor, S. Verdu, "Single-User Detectors for Multiuser Channels," *IEEE Transactions on Communications,* Vol. 36. No. 1, January 1988.
- 63 A. Elezabi, A. Duel-Hallen, "Post-Decoding Interference Cancellation for Coded CDMA System," *Proc. of IEEE Int. Symp. on Info. Theory,* p. 282, Aug. 1998.
- 64 T. O'Farrel, "An Optimum Single-User Detector for Asynchronous DS/CDMA Radio Based System", *IEEE ISSSTA '96 Conference. Pp. 1029-1033, Sept. 1996.*
- 65 P. R. Patel, J. M. Holtzman, "Analysis of a DS/CDMA Successive Interference Cancellation Scheme Using Correlations," *IEEE Globecom,* Pp. 76-80, 1993.
- 66 M. B. Pursley, "Spread Spectrum Multiple Access Communications," *CISM Courses and Lectures No. 265, Springer-Verlag Wien, New York, 1981.*
- 67 CAPSIM, XCAD Corporation, Cary, NC, www.xcad.com, 1989-2000.

